

From First Stars to the Spite Plateau: a Possible Reconciliation of Halo Stars Observations with Predictions from Big Bang Nucleosynthesis.

L. Piau ¹

University of Chicago, LASR 933, East 56th street, and JINA: Joint Institute for Nuclear Astrophysics, Chicago, IL, 60637, USA

laurent@oddjob.uchicago.edu

T. C. Beers²

Department of Physics & Astronomy, CSCE: Center for the Study of Cosmic Evolution, and JINA: Joint Institute for Nuclear Astrophysics, Michigan State University, East Lansing, MI 48824, USA

beers@pa.msu.edu

D.S. Balsara ³

Department of Physics, University of Notre Dame, 225 Nieuwland Science Hall, Notre Dame, IN, 46556, USA

dbalsara@nd.edu

T. Sivarani⁴

Department of Physics & Astronomy, CSCE: Center for the Study of Cosmic Evolution, and JINA: Joint Institute for Nuclear Astrophysics, Michigan State University, East Lansing, MI 48824, USA

thirupathi@pa.msu.edu

J. W. Truran ⁵

University of Chicago, Department of Astronomy & Astrophysics, 933, East 56th street, Chicago, IL, 60637, USA Argonne National Laboratory, 9700 South Cass Road, Argonne, IL, 60439-4863, USA

truran@nova.uchicago.edu

and

J. W. Ferguson ⁶

Physics Department Wichita State University Wichita, KS 67260-0032, USA

jason.ferguson@wichita.edu

ABSTRACT

Since the pioneering observations of Spite & Spite in 1982, the constant lithium abundance of metal-poor ($[\text{Fe}/\text{H}] < -1.3$) halo stars near the turnoff has been attributed to a cosmological origin. Closer analysis, however, revealed that the observed abundance lies at $\Delta^7\text{Li} \sim 0.4$ dex below the predictions of Big Bang Nucleosynthesis (BBN). The measurements of deuterium abundances along the lines of sight toward quasars, and the recent data from the Wilkinson Microwave Anisotropy Probe (WMAP), have independently confirmed this gap. We suggest here that part of the discrepancy (from 0.2 to 0.3 dex) is explained by a first generation of stars that efficiently depleted lithium. Assuming that the models for lithium evolution in halo turnoff stars, as well as the $\Delta^7\text{Li}$ estimates are correct, we infer that between one-third and one-half of the baryonic matter of the early halo (i.e. $\sim 10^9 M_\odot$) was processed through Population III stars. This new paradigm proposes a very economical solution to the lingering difficulty of understanding the

1. Introduction

For more than 20 years lithium has been recognized as an efficient probe of the (early) nucleosynthetic evolution of the Universe. The abundance of ${}^7\text{Li}$ in halo stars is almost independent both of their effective temperatures (between 6400 K and 5600 K) and of their metallicity between $[\text{Fe}/\text{H}] = -1.5$ and -2.5 . This observational fact was first discovered in the early 1980s by Spite & Spite (1982), and has been confirmed by numerous observational studies of increasing accuracy in the subsequent decades, including : Hobbs & Duncan (1987); Rebolo, Beckman, & Molaro (1988); Spite & Spite (1993); Thorburn (1994); Molaro, Primas, & Bonifacio 1995; Ryan et al. (1996); Bonifacio & Molaro (1997); Ryan, Norris, & Beers (1999); Bonifacio et al. (2002); Asplund et al. (2006); Bonifacio et al. (2006). The most natural way to understand the apparently constant ${}^7\text{Li}$ abundance on the so-called Spite Plateau is to relate it directly to production by Big Bang Nucleosynthesis (hereafter BBN). BBN is understood to produce ${}^7\text{Li}$ and the other light species ${}^2\text{H}$, ${}^3\text{He}$ and ${}^4\text{He}$. One clear challenge to this simple picture is the fact that the observed abundances of ${}^7\text{Li}$ in the atmospheres of halo stars are clearly below the predictions of standard BBN.

On average, the measurements of ${}^2\text{H}$ in intergalactic clouds along the lines of sight to quasars are $({}^2\text{H}/\text{H})_{\text{p}} \sim 3 \times 10^{-5}$ (O’Meara et al. 2001; Burles 2002 and references therein). Strictly speaking, this estimate is only a lower limit on the primordial ${}^2\text{H}$, as, except for the Big Bang, there is no astrophysical site currently known to significantly produce ${}^2\text{H}$. However, the ${}^2\text{H}$ observed towards QSOs (in a medium where the metallicity is below $[\text{Fe}/\text{H}] = -1.0$) is probably very close to the actual primordial value; for various assumptions, the early Galactic disk chemical evolution models predict no significant change of ${}^2\text{H}$ as long as $[\text{O}/\text{H}] < -0.5$ (Romano et al. 2006). 3×10^{-5} is presumably the deuterium-to-hydrogen ratio left behind by BBN. In order to have provided such a deuterium fraction, standard BBN would have to have produced much more lithium than is currently observed in halo stars on the Spite Plateau. More recently, the validity of this discrepancy related to lithium found further strong support through the con-

straints provided by the cosmic radiation background anisotropies measured by the Wilkinson Microwave Anisotropy Probe (WMAP). These anisotropies imply a baryon number $\eta_{\frac{b}{\gamma}}$ around 6×10^{-10} (Spergel et al. 2003). In the context of standard BBN, using the most recent compilation of nuclear reaction rates, this $\eta_{\frac{b}{\gamma}}$ implies a primordial deuterium fraction in perfect agreement with the ${}^2\text{H}$ observations in intergalactic clouds, but a ${}^7\text{Li}$ abundance (hereafter referred as $A({}^7\text{Li}) = 12 + \log[\text{N}(\text{Li})/\text{N}(\text{H})]$) much higher than what is observed in halo stars. It is also interesting to note that these BBN predictions are robust with respect to constraints on the nuclear cross sections evaluated on the basis of solar neutrinos (Cyburt et al. 2004), and also with respect to recent estimates of primordial ${}^4\text{He}$ (Olive & Skillman 2004; Cyburt et al. 2005). The current situation is therefore the following. On the one hand, the present estimate of primordial $A({}^7\text{Li})$, based on the most up-to-date nuclear physics, seems reliably set at $A({}^7\text{Li}) = 2.6$ (Coc et al. 2004). On the other hand, the observed halo-star lithium plateau appears to be no larger than $A({}^7\text{Li}) = 2.1 - 2.2$, although Meléndez & Ramirez (2004) have argued that changes in the adopted temperature scale might be able to raise the observed Spite Plateau value of $A({}^7\text{Li})$ up to 2.4. Fields, Olive, & Vangioni-Flam (2005) point out that the revision in the temperature scale suggested by Meléndez & Ramirez (2004) raises several serious challenges to Galactic cosmic-ray nucleosynthesis and Galactic chemical evolution, and hence must be considered with caution.

Lithium is known to be a very fragile element, one that is rapidly destroyed by nuclear reactions in stellar interiors when the temperature exceeds 2.5×10^6 K. One possible explanation of the discrepancy between the expected primordial lithium and that measured on the Spite Plateau could therefore be that the lithium presently observed in the outer atmospheres of halo stars has been depleted by stellar-evolution processes over the long history of the Galaxy. A great number of modeling efforts have investigated this hypothesis (as recently summarized by Charbonnel & Primas 2005). As far as we are aware, these previous works have only addressed the question of whether the halo stars themselves could be responsible for *in situ* lithium depletion during

their main-sequence (hereafter MS) or pre-main-sequence (hereafter pre-MS) evolution.

In this paper we address the question of the early evolution of lithium from a different perspective, and examine the possible effects of zero-metallicity or near zero-metallicity (Population III) stars on the abundance of lithium in the interstellar medium from which (by definition) the next-generation stars formed. Indeed, no halo star is presently observed that is completely devoid of elements that were formed post-Big Bang, such as C, N, O, the α -elements, and the iron-peak elements. Hence, all of the recognized halo stars must have formed from material that was enriched – at least partially – by a Population III object or a subsequent stellar generation. If the heavier-than-lithium element fractions of Spite Plateau stars have been affected, then it stands to reason that their lithium abundances may have been altered as well, in particular if the Population III stars are capable of destroying lithium, and efficiently recycling this Li-depleted gas back into the interstellar medium (hereafter ISM). In this scenario, other elements, as well as the trends and observed scatter of other elements, should have been affected too. These possibilities are considered in turn below.

Implicit in the above scenario for ${}^7\text{Li}$ destruction is the assumption that the ${}^7\text{Li}$ -depleted ejecta from massive Population III stars are efficiently mixed with the proto-Galactic ISM. A static ISM would not permit efficient mixing. However, several lines of evidence, cataloged in later sections, suggest that the proto-Galactic ISM was in fact quite dynamic. Recent observations of distant ultraluminous infrared galaxies (ULIRGs) (Shapley et al. 2001; Daddi et al. 2005; Yan et al. 2005) show that a significant amount of star formation might have taken place as early as $z \sim 6$. Numerical simulations of Λ -dominated cold dark matter cosmologies (Nagamine et al. 2004; Night et al. 2005) also support scenarios where galaxies form early. Furthermore, they support scenarios where larger systems formed via the coalescence and mergers of smaller systems, a scenario that also finds some observational support (Dasyra et al. 2006). Thus, several lines of evidence indicate that proto-galactic ISMs were dynamically evolving due to massive Population III star formation or mergers in the early Universe. Perhaps the best evidence to indicate that our Galaxy might also

have passed through such a phase of evolution emerges from the small scatter in α -capture elements that has been observed in very metal-poor halo dwarfs down to $[\text{Fe}/\text{H}] \sim -2$ (Norris et al. 2001, and references therein). The fact that a wide range of α -capture elements have evolved in lock-step with $[\text{Fe}/\text{H}]$, and presently exhibit extremely small observed scatter about well-defined trends with $[\text{Fe}/\text{H}]$, suggests that massive stars not only produced these elements, but also that the winds and Type II SNe from these stars were very efficient at dispersing metals throughout the proto-Galactic ISM. Below $[\text{Fe}/\text{H}] \sim -2$ the halo stars still exhibit a small scatter in α -capture or iron-peak elements (Cayrel et al. 2004; Arnone et al. 2005). However, the r-process elements seem to be more scattered (Truran et al. 2002), which makes an efficient mixing of the ISM less probable in these metallicity regimes. Studies of supernova-driven mixing of the ISM have already been presented in the literature (Korpi et al. 1999; Avillez & Breitschwerdt 2004; Balsara et al. 2004; Balsara & Kim 2005; Mac Low et al. 2005). We draw on the insights available from the literature to understand the dispersal of lithium-depleted but metal-enriched material throughout an early ISM.

For discussion of the lithium discrepancy, we focus on the metal-poor stars with effective temperatures above 6000 K. These objects are less likely to have undergone significant lithium depletion themselves, at least as compared to their cooler counterparts, due to the smaller outer convection region with increasing mass (and hence temperature). In §2 we address the question of whether or not these main-sequence-turnoff stars could have depleted a substantial fraction of their initial lithium content when non-standard mixing processes are considered (in addition to convection, microscopic diffusion and gravitational settling). We find that these stars probably experienced a moderate lithium depletion of their surface abundances (~ 0.2 to 0.4 dex). Section 3 discusses the possible role that Population III stars might have played. We estimate that between one-third and one-half of the Galactic halo matter must have been processed through these stars in order to explain the identified discrepancy between the lithium plateau observations and the predicted level of primordial BBN lithium production. We emphasize that this derived fraction is

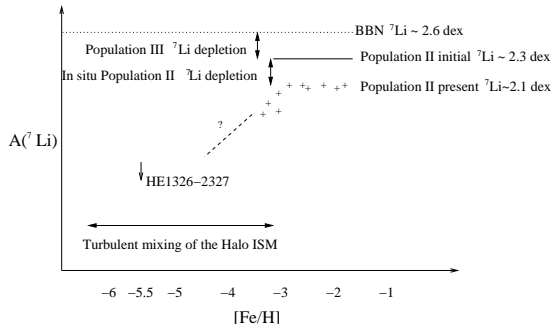


Fig. 1.— A schematic of the ${}^7\text{Li}$ vs. $[\text{Fe}/\text{H}]$ relationship and the evolution of the ${}^7\text{Li}$ abundance we propose occurred in the early halo. The dotted-line shows the BBN ${}^7\text{Li}$ abundance. The solid line shows the initial Population II ${}^7\text{Li}$ abundance. The crosses show the abundance in ${}^7\text{Li}$ presently observed in the halo. The dashed-line is indicative of a possible decrease in the ${}^7\text{Li}$ abundance from the apparent edge of the Spite Plateau around $[\text{Fe}/\text{H}] \sim -2.5$ to objects similar to HE 1327-2326.

a result of our modeling, and not an input assumption. To arrive at this conclusion, we make the assumptions: (a) $A({}^7\text{Li})$ from BBN is 2.6, (b) the level of observed Spite Plateau lithium is between 2.1 and 2.2 for main-sequence-turnoff stars with metallicity above $[\text{Fe}/\text{H}] = -2.5$, and (c) that present models of Population II stars correctly predict the likely amount of *in situ* lithium depletion in these stars. In §4 we discuss interesting new lithium trends that have been observed for halo stars below $[\text{Fe}/\text{H}] = -2.5$. In §5 we present arguments in support of the likelihood of efficient early mixing of the ISM due to turbulent mixing by early supernovae. Figure 1 summarizes the general features of our model describing lithium history, from the BBN to present observations in the halo. Note that this Figure indicates the presence of two distinct contributions to primordial lithium depletion in order to reach the presently observed Spite Plateau value of lithium abundance.

In §6 we summarize other recent observations that might be explained by the scenario we propose, including (a) the unique abundance patterns observed among stars of the lowest metallicity, (b) the production of primary nitrogen and the observed trends of C/O and N/O in very low-metallicity stars, (c) the lack of observed star-to-

star scatter in alpha- and iron-peak elements in stars of very low metallicity, (d) the peculiar features of carbon in extremely-metal-poor stars and hyper metal-poor stars¹. Our conclusions and discussion follow in §7, where we also suggest several testable predictions of the Population III processing model. The reader who is only interested in the main idea of this article might read §3 and §4, and then directly move to the conclusions presented in §7.

2. Lithium Evolution in Very Metal-Poor Stars

Several observed facts about the nature of the Spite Plateau are of central importance for testing our Li-astration model. The lithium plateau is flat only as a first approximation. Ryan et al. (1996) have argued for the presence of small, but significant, correlations in $A({}^7\text{Li})$ with both effective temperature (+0.04 dex per 100 K) and with metallicity (+0.11 dex per dex). In an effort to avoid any correlations with temperature, Ryan et al. (1999) investigated a sample of 23 halo dwarfs with similar T_{eff} (between 6100 K and 6300 K), and obtained a slope of $A({}^7\text{Li})$ with respect to $[\text{Fe}/\text{H}]$ of +0.12 dex per dex, quite similar to the previous analysis. This slope was suggested by Ryan et al. (2000) to be the signature of lithium production by spallation (see Fields & Olive 1999) from cosmic rays and the supernova ν -process (Woosley et al. 1990; Woosley & Weaver 1995), which gradually increase the lithium content of the interstellar medium from which successive generations of stars formed. Recent observational results suggest that the slope of $A({}^7\text{Li})$ with $[\text{Fe}/\text{H}]$ sharply changes below $[\text{Fe}/\text{H}] \sim -2.5$ (Asplund et al. 2006). In this very low-metallicity regime the increase of the lithium fraction with metallicity seems more rapid, as shown by Figure 2. It is also possible that the scatter of $A({}^7\text{Li})$ similarly goes up below this metallicity (Bonifacio et al. 2005, 2006). The star-to-star scatter in measured $A({}^7\text{Li})$ for metal-poor stars on the plateau is *extremely* small, on the order of 0.03-0.05 dex (Ryan et al. 1999; Asplund et al. 2006; Bonifacio

¹Following the taxonomy suggested by Beers & Christlieb (2005), the extremely metal-poor star term refers to stars with $[\text{Fe}/\text{H}] < -3$, while the hyper metal-poor star term refers to the stars with $[\text{Fe}/\text{H}] < -5$.

et al. 2006), well within the expected observational errors² However, Figure 2 suggests a possible increase in the scatter of $A(^7\text{Li})$ below $[\text{Fe}/\text{H}] \sim -2.5$. Clearly, these new features concerning the break in the the slope and increased scatter of the Spite Plateau for very low-metallicity stars require verification based on measurements of lithium abundances for additional larger samples of stars with extremely low metallicity. We remark that the tendency for the lithium fraction to decrease strongly in (at least some) dwarfs below $[\text{Fe}/\text{H}] \sim -2.5$ is confirmed by high-resolution observations of the the hyper metal-poor star HE 1327-2326, where an upper limit for $A(^7\text{Li})$ of 1.5 dex is obtained (Frebel et al. 2005; Aoki et al. 2006a). Very recent results, yet to be published, further show that $A(^7\text{Li}) < 0.9$ should be adopted in HE 1327-2326 (A. Frebel, private communication).

We now consider the evolution of lithium abundances for extremely metal-poor turnoff stars with $[\text{Fe}/\text{H}] = -3.5$ having the typical distribution of metals associated with most halo stars (hereafter composition A): $[\alpha/\text{Fe}] = +0.35$, where α stands for oxygen and the α elements (Ne, Mg, Si, S, Ar, Ca, and Ti), while $[\text{C}/\text{Fe}] = [\text{N}/\text{Fe}] = 0$ (see Piau 2006 for details). Similarly, we consider the lithium abundance evolution in stars with the same composition as HE 1327-2326 (hereafter composition B) which, with $[\text{Fe}/\text{H}] = -5.5$ is the most iron-poor star presently known (Frebel et al. 2005). HE 1327-2326 has a rather unique composition, and in particular exhibits huge carbon, nitrogen, and oxygen content with respect to its iron content. Depending on the (still unclear) evolutionary status of this star, $[\text{O}/\text{Fe}]$ lies between $+2.8 \pm 0.2$ (subgiant) and $+2.5 \pm 0.2$ (dwarf), while $[\text{C}/\text{Fe}] = +4.1$ (Frebel et al. 2006). Both of the compositions we model are assumed to have the primordial helium mass fraction $Y_p = 0.2479$, as well as primordial ^7Li and ^2H number fractions of 4.15×10^{-5} ($A(^7\text{Li}) = 2.6$) and 2.60×10^{-5} respectively, as estimated by Coc et al. (2004). The modeling of the evolution of ^7Li abundances

²We note that debate continues on whether or not the Spite Plateau exhibits a slope (on the order of 0.1-0.2 dex per dex) in $A(^7\text{Li})$ vs. $[\text{Fe}/\text{H}]$, with several authors coming out in favor of such a slope (Ryan et al. 1999; Asplund et al. 2006), and others not (Meléndez & Ramirez 2004; Bonifacio et al. 2006).

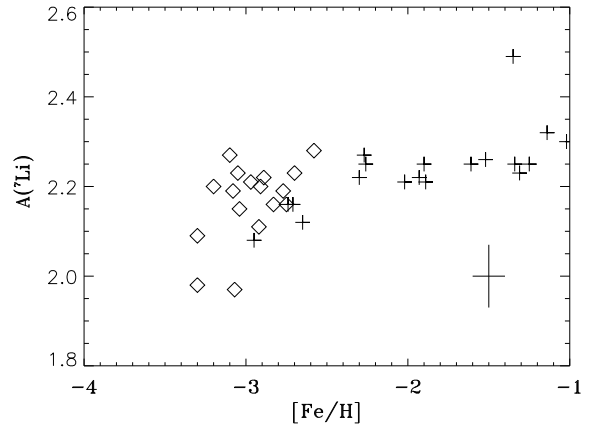


Fig. 2.— $A(^7\text{Li})$ measurements among the very low-metallicity halo turnoff stars. Crosses: data from Asplund et al. (2006), Diamonds: data from Bonifacio et al. (2006). The abundances from the two samples assume the same T_{eff} scale, so they can be compared directly. The error bars shown on the lower right represent the (comparable) uncertainties on $[\text{Fe}/\text{H}]$ and $A(^7\text{Li})$ from both studies. Three very low-metallicity stars from Bonifacio et al. (2006) clearly appear below the plateau.

is performed herein using the stellar evolution code CESAM (Morel 1997). The general inputs to the code (equation of state, opacities, convection modelling, etc.) are similar to the description provided in Piau (2006), and we do not repeat them here.

Table 1 summarizes the initial compositions we have adopted in our models. In the case of HE 1327-2326 all of the initial metal abundances were increased by ~ 0.2 dex in order to roughly take into account the microscopic diffusion and gravitational settling of heavy elements (therefore $[\text{Fe}/\text{H}] = -5.3$ initially) during the main-sequence evolution (hereafter MS) of halo dwarfs. Because of its very thin outer convection zone, it is probable that HE 1327-2326 experienced a stronger diffusion and settling of the heavy elements than a typical halo star. Thus, we also constructed a model of HE 1327-2326 where the initial $[\text{Fe}/\text{H}]$ is increased to -4.5 (see below). Because of the small impact of metals on the Equation of State (EOS) in the Population II regime, the main difference in the modeling between the typ-

Table 1: Initial Metal Fractions Relative to $[\text{Fe}/\text{H}]$ Adopted in our Models

Metal	“Typical” Halo Star	HE 1327-2326
	Composition A	Composition B
$[\text{C}/\text{Fe}]$	0	+3.9
$[\text{N}/\text{Fe}]$	0	+4.2
$[\text{O}/\text{Fe}]$	0.35	+2.6
$[\text{Fe}/\text{H}]$	−3.5	−5.3
Y, Z	0.2479, 9.77×10^{-6}	0.2479, 2.98×10^{-4}

NOTE.—We adopt the Grevesse & Noels (1993) solar composition to infer absolute abundances. Note that the accuracy on heavy element abundances for HE 1327-2326 are on the order, or larger, than the change of abundances resulting from the revision of the solar composition by Asplund et al. (2006). Y and Z stand, as usual, for the total mass fractions in helium and the heavy elements.

ical halo-stars’ composition and that of HE 1327-2326 relies on the opacities. The required opacities have been taken from the OPAL web site (<http://www-phys.llnl.gov/Research/OPAL/>) for halo-star composition (the α -element-enhanced table of F. Allard) or alternatively, generated online on this site for HE 1327-2326. The low-temperature opacities ($\log T < 3.75$) were generated by one of the authors (see Ferguson et al. 2005). In order to achieve $T_{\text{eff}} = 6200$ K at an age of 13.5 Gyr, we predict the mass of HE 1327-2326 to be $0.41 M_{\odot}$. This is much smaller than the mass of a similar-temperature and similar-age star with the typical composition of an extremely metal-poor halo star having $[\text{Fe}/\text{H}] = -3.5$: $0.69 M_{\odot}$. It is well known that the effective temperature strongly increases, at a given mass and age, when the metallicity decreases. More precisely, this effect is related to the drop of abundance of the metals having low-energy first-ionization potentials, such as Na, Ca, and Fe (e.g., Gehren et al. 2004). The less numerous these metals, the less abundant the H^- ion, and the smaller the atmospheric opacity. In the case of HE 1327-2326, this trend is reinforced by the presence of a convective core associated with ^{12}C to ^{14}N conversion during most of the MS phase. The combination of the low luminosity and the high initial carbon fraction allows this convective core (induced by CN-cycle burning) to survive to the age of 15 Gyr, which is

when we stop our computations. Due to the convective core in models with HE 1327-2326 composition, they live longer on the MS than typical halo stars. The impact of a C-burning convection zone on the MS lifetime has been mentioned in previous stellar evolution studies (e.g., Maeder & Meynet 1989). More generally, the increasing size of the central regions lengthens the MS duration, because they increase the amount of available hydrogen fuel (see, e.g., Schaller et al. 1992). Table 2 shows the main properties of our $T_{\text{eff}} \sim 6200$ K models at 13.5 Gyr. Because stars with similar composition to HE 1327-2326 may be detected in the near future, Figure 3 shows comparative isochrones of this peculiar-composition star as compared to typical extremely metal-poor halo stars.

Lithium is a fragile element, and therefore it can be destroyed even in the envelopes of low-mass stars. It is difficult to accurately model its history, mainly because it probably depends on non-convective mixing mechanisms, as suggested by the lithium evolution of solar-like stars. The observational facts are: (1) lithium has been depleted in the Sun by a factor ~ 160 (Asplund et al. 2005), and (2) there appears to be depletion in solar analogs on a timescale of a few hundred Myr, as shown by studies of Galactic open clusters (Sestito & Randich 2005). This depletion occurs in objects having, as does our Sun, the base of their

Table 2: Initial Mass, Effective Temperature, Temperature at the Base of the outer Convection Zone, Mass of Outer Convection Zone, Bolometric Luminosity, Surface Gravity, and Central Hydrogen Mass Fraction (X_c) for Objects of the Two Compositions Considered

Composition	Mass (M_\odot)	T_{eff} (K)	T_{BCZ} (K)	M_{CZ} (M_\odot)	$L(L_\odot)$	$\log g$	X_c
A	0.69	6194	1.2×10^6	4.5×10^{-3}	0.675	4.57	0.14
B	0.41	6197	4.8×10^5	2.9×10^{-4}	0.220	4.83	0.54

NOTE.—The presence of a convective core translates into a much higher X_c in the case of composition B (HE 1327-2326). We do not take into account the possibility of core-convection overshooting; this mechanism would increase X_c even further.

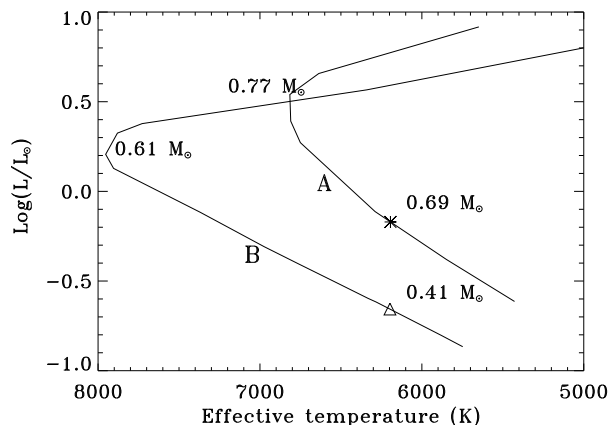


Fig. 3.— Comparative isochrones at 13.5 Gyr for compositions A and B models without diffusion. The positions and masses of the objects exhibiting the present HE 1327-2326 T_{eff} are indicated by a triangle and a star on each isochrone. The turnoff masses on each isochrone are also indicated.

convection zones (hereafter BCZ) at temperatures below 2.5×10^6 K, and therefore is related to non-standard mixing processes in the sense that they are not the signature of convection only, but must involve rotation effects, magnetic effects, or internal wave-induced mixing. Our computations include two possible non-standard mixing processes. The first is the so-called tachocline mixing process (Spiegel & Zahn 1992). This rotationally-induced mixing occurs in a thin layer below the convection zone. It correctly predicts the timescale for ^7Li de-

pletion as seen in Galactic open clusters (Brun et al. 1999; Piau et al. 2003) as well as the amount of ^7Li depletion in the Sun. Moreover, this process preserves the initial solar ^9Be , and provides better agreement between the theoretical solar sound-speed profile and that inferred from helioseismology (Brun et al. 1999). There are two important parameters in the tachocline modeling: (1) the assumed width of the tachocline region, which we take to be 2.5% of the stellar radius, based on solar seismic measurements (Corbard et al. 1999, Charbonneau et al. 1999), and (2) the buoyancy frequency assumed in the tachocline region, which we assume to be $10 \mu\text{Hz}$ (for discussion about these choices we refer the reader to Piau et al. 2003). Next, one needs to introduce the rotation history into the modeling. Since this history is unknown in Population II stars, we assume it is similar to the Population I low-mass objects. We consider that the star rotates as a solid at all times, and that the initial rotation period is 8 days. Despite the contraction we assume the angular velocity remains unchanged during the first million years of evolution, because the star is coupled to its early circumstellar disk. Past this age the star spins up. The angular momentum is roughly constant, but the object continues to contract. After the Zero-Age Main-Sequence (ZAMS) stage, it slows down through the effect of magnetic wind braking. We follow the prescriptions given by Kawaler (1988) on the losses of angular momentum, J :

$$\frac{dJ}{dt} = -K\Omega^3, \text{ if } \Omega < \Omega_{\text{sat}} \text{ and } \frac{dJ}{dt} = -K\Omega\Omega_{\text{sat}}^2, \text{ if } \Omega > \Omega_{\text{sat}} \quad (1)$$

In the above, Ω is the angular velocity, Ω_{sat} is a saturation threshold in angular velocity, and K is a constant. The parameter Ω_{sat} is set to $14\Omega_{\odot}$, following the observations of the rotation history of solar analogs in open clusters (Bouvier, Forestini, & Allain 1997). The constant K is either adjusted to $2.0 \times 10^{46} \text{ g s cm}^2$ (composition A and $0.69 M_{\odot}$ star) or $8.5 \times 10^{45} \text{ g s cm}^2$ (composition B and $0.41 M_{\odot}$ star) in order to let our models rotate at 30 km/s at the Hyades age (~ 625 Myr). This is the velocity assessed by Gaigé (1993) from observations of objects having $T_{\text{eff}} \sim 6200$ K in this cluster. The impact of the combined microscopic diffusion gravitational settling and tachocline mixing have been explored in detail by Piau (2006) for halo stars of metallicity $[\text{Fe}/\text{H}] = -2.0$. These models indicate that lithium depletion at the MS turnoff for the Spite Plateau is ~ 0.2 dex. In the case of ${}^7\text{Li}$, this depletion always occurs because of microscopic diffusion, not through nuclear destruction. However, in the case of ${}^6\text{Li}$ and $0.69 M_{\odot}$ models of composition A, some nuclear destruction occurs.

The other possibility we explore for non-standard mixing is the prescription adopted by Richard, Michaud, & Richer (2005). Following these authors, we have added turbulent mixing below the convection zone with a turbulent diffusion coefficient D_t :

$$D_t = 400 D_{\text{He}}(T_o) \frac{\rho(T_o)^3}{\rho} \quad (2)$$

where $D_{\text{He}}(T_o)$ and $\rho(T_o)$ are, respectively, the helium microscopic diffusion coefficient and density in a star at $T_o = 10^6$ K. This turbulent mixing law is the most satisfactory one among the various prescriptions for turbulent mixing explored by Richard et al. (2005), in the sense that it produces the best agreement to the features of the lithium Spite Plateau without inducing ${}^6\text{Li}$ depletion. This point is now supported by the recent observations of ${}^6\text{Li}$ on the Spite Plateau (Asplund et al. 2006). Similar to the models of Piau (2006), the results from Richard et al. (2005) suggest that the lithium depletion is around 0.2 dex near the MS turnoff for the turbulent mixing law of equation 2.

Table 3 lists our results for both the extremely metal-poor Population II star (composition A)

and for HE 1327-2326 (composition B). The masses of the stars ending up with the required effective temperature at 13.5 Gyr slightly depend on the diffusion processes that are taken into account. For instance, a model of a given mass ends up with a smaller effective temperature when the microscopic diffusion and gravitational settling are taken into account than when they are not. For this reason the models in Table 3 correspond to a small range of masses. In both composition A and B models no pre-MS ${}^6\text{Li}$ or ${}^7\text{Li}$ depletion is expected if we consider the objects now at 13.5 Gyr and having $\sim T_{\text{eff}} = 6200\text{K}$. Subsequently, a MS depletion occurs, on the order of 0.06 dex to 0.8 dex for ${}^7\text{Li}$. Similar to what happens on the Spite Plateau stars near the turnoff, this is a diffusion and settling effect, and not the result of nuclear destruction from deep mixing because, as illustrated in Table 2, the temperature near the BCZ is well below the ${}^7\text{Li}$ destruction temperature. The BCZ temperature is moreover unaffected by the turbulent mixing prescription below the convection zone. A few additional remarks need to be made:

For composition A: ${}^6\text{Li}$ evolves during MS because of nuclear destruction, in contrast to ${}^7\text{Li}$. For these models the base of the outer convection zone lies close enough to the regions where the temperature exceeds 2×10^6 K, and material is dragged down to these regions by non-standard mixing. Indeed, $T_{\text{BCZ}} = 1.5 \times 10^6$ K at 8 Gyr, and this temperature decreases slowly towards the end of the MS to the value reported in Table 2. The depletion therefore is stronger for ${}^6\text{Li}$ than it is for ${}^7\text{Li}$.

For composition B: the depletion is slightly less important for ${}^6\text{Li}$ than for ${}^7\text{Li}$, as ${}^7\text{Li}$ is heavier, and the depletion results not only from microscopic diffusion but also from gravitational settling for both isotopes. Moreover, the tachocline mixing models that do not include the microscopic diffusion and gravitational settling show ~ 0.6 dex more ${}^7\text{Li}$ than those that include these effects. This is a hint that the microscopic diffusion and gravitational settling and their interplay with the turbulence must be carefully taken into consideration in future studies of hyper metal-poor stars. As the evolution of ${}^7\text{Li}$ suggests that the heavy-element surface abundances could have dropped significantly during the lifetime of HE 1327-2326,

we also computed a model of this star starting with $[\text{Fe}/\text{H}] = -4.5$ and $[\text{X}/\text{Fe}]$ values otherwise identical to table 1. This model includes the diffusion and tachocline mixing effects. Its ${}^7\text{Li}$ and ${}^6\text{Li}$ chemical abundances at 13.5 Gyr and are very similar to what is reported in table 3 with $A({}^7\text{Li}) = 1.81$ and $A({}^6\text{Li}) = 0.42$.

HE 1327-2326 is not the first metal-poor halo turnoff star that is also lithium poor. Indeed, similar objects have been known for some time (Ryan et al. 2002). They represent between 5 % and 10 % of the Spite Plateau stars. However, these objects have iron abundances that are much higher than HE 1327-2326, and rotate faster than typical Spite Plateau stars (Ryan & Elliott 2005). Moreover, they generally belong to binary systems: three out of four of these Li-poor stars in the Ryan et al. (2002) sample are confirmed binaries, with the secondary suspected to be a compact object. A fourth member of the Ryan et al. Li-poor sample of stars, CD-31:19466, however, does not presently appear as a binary or as a fast rotator. In this respect, it is comparable to HE 1327-2326 because of its low lithium abundance, despite having a much higher iron content. In the other Li-poor objects, binarity and rotation suggest that the surface composition and angular momentum might have been affected by accretion from the companion (see Piau 2006 for a discussion). This is in contrast to HE 1327-2326 where we note that the rotation is presently estimated to be similar to the lithium plateau stars and no clues of binarity have been detected so far (Aoki et al. 2006a; Frebel et al. 2006).

In conclusion, it is very unlikely that HE 1327-2326, as well as a $T_{\text{eff}} = 6200\text{K}$ and composition A object have decreased by more than an order of magnitude their initial surface lithium in the course of their evolution. HE 1327-2326 most probably exhibits its pristine abundance to within 0.8 dex. For a composition A object at $T_{\text{eff}} = 6200\text{K}$, the ${}^7\text{Li}$ depletion we compute is 0.4 dex at most. This conclusion is unchanged for reasonable age or effective temperature variations. The results displayed in Table 3 are rather insensitive to age uncertainties: a change from 13.5 to 11.5 Gyr in the age of the models would increase $A({}^6\text{Li})$ or $A({}^7\text{Li})$ by less than 0.2 dex in any of the cases considered. Similarly, a slightly incorrect measurement of T_{eff} would not change

the global picture – an error of 100 K in T_{eff} translates to an error of ~ 0.06 dex on $A({}^7\text{Li})$ for the considered metallicity and effective temperature range (P. Bonifacio, private communication). Models with effective temperatures slightly above or below 6200 K would not change the results either. For instance, in the case of models including microscopic diffusion, gravitational settling, and tachocline diffusion, but with $T_{\text{eff}}=6000\text{K}$, $A({}^7\text{Li})=2.22$ and 1.82 at 13.5 Gyr for composition A and B, respectively. The variations of $A({}^7\text{Li})$ with T_{eff} are smooth around the turnoff. Interestingly, in the study of Bonifacio et al. (2006), the star CS 22948-093 ($T_{\text{eff}} = 6356\text{K}$, $[\text{Fe}/\text{H}] = -3.30$) appears to have $A({}^7\text{Li}) = 1.98$, slightly below the lithium plateau, estimated to be around $A({}^7\text{Li}) = 2.17$ by these authors. This star could be compared to our composition A and $0.69M_{\odot}$ models. Its observed ${}^7\text{Li}$ abundance is at least 0.3 dex below our predictions, which also suggests that this extremely metal-poor star inherited its initial lower lithium fraction from its progenitor cloud.

3. Lithium Depletion and Astaration in Population III stars

In the model we are exploring, the presently observed lithium abundance for metal-poor stars on the Spite Plateau represents (or nearly represents) the composition of the ISM out of which these low-mass stars originally formed (as shown in §2). If we posit that the original composition of the ISM from which high-mass zero-metallicity stars formed is that given by predictions of BBN, then we must look to such progenitor stars as the source of not only the initial iron and other elements among subsequently formed low-mass stars, but we must also consider the consequences on the lithium abundance of the ISM after these stars have ejected their processed material.

Using the CESAM code, we have constructed standard models of stars totally devoid of metals in the 1 to 40 M_{\odot} mass range. The hydrogen mass fraction is set to 0.75 and, correspondingly, the helium fraction is set to 0.25. Neither rotation nor diffusion effects are considered. The models are evolved until the central temperature reaches 10^8K , or the age is 100 Myr, whichever comes

Table 3: Initial Lithium Isotope Abundances From Turbulent Mixing Models

Composition and Mass Range	Microscopic Effects & Tachocline Diffusion	No Microscopic Effects and Tachocline Diffusion	Microscopic Effects and “Richard” Diffusion
A, 0.69-71 M_{\odot}	${}^7\text{Li}=2.38$, ${}^6\text{Li} = -0.01$	${}^7\text{Li}=2.54$, ${}^6\text{Li}=0.06$	${}^7\text{Li}=2.26$, ${}^6\text{Li}=0.00$
B, 0.41-43 M_{\odot}	${}^7\text{Li}=1.83$, ${}^6\text{Li}=0.44$	${}^7\text{Li}=2.52$, ${}^6\text{Li}=1.02$	${}^7\text{Li}=1.96$, ${}^6\text{Li}=0.54$

NOTE.—The masses of the models achieving $T_{\text{eff}} = 6200$ K at 13.5 Gyr vary slightly as a function of the diffusion processes considered. The models including the microscopic, gravitational settling, and tachocline diffusion are the heaviest ones, with 0.71 and 0.43 M_{\odot} for composition A and B, respectively. The models without microscopic diffusion and gravitational settling are the lightest ones, with 0.69 and 0.41 M_{\odot} for composition A and B, respectively. Microscopic effects include microscopic diffusion and gravitational settling. The “Richard” diffusion refers to the turbulent diffusion explained in the text. All of the models were started with $A({}^7\text{Li}) = 2.6$ and $A({}^6\text{Li}) = 1.1$

first³. We are not interested here in the evolutionary effects associated with these Population III objects, but on their ability to deplete their initial lithium content. The outer layers of the Population III stars we model are radiatively stable, or for lower-mass models, they exhibit very shallow outer convective regions. For example, the 1 M_{\odot} model exhibits convective instability over only the outer 0.75% of its radius. Thus, the material present in the outer regions of such stars will, *a priori*, not be exposed to temperatures above the lithium depletion temperature of 2.5×10^6 K. Figure 4 shows the fractional mass, $f_{7\text{Li}}$, where lithium is preserved as a function of the total mass of the star. To evaluate these stellar mass fractions, we simply considered regions of the star with temperature below 2.5×10^6 K. As in finite-metallicity stars, Population III stars clearly destroy most of their initial ${}^7\text{Li}$. This trend increases with increasing mass.

The global impact on ${}^7\text{Li}$ in the generation of stars that directly follow the very first generation will depend on the initial mass function (hereafter IMF) of these first stars. Following Ballero et al. (2005), we assume the IMF of Population III stars

is:

$$\phi(m) \propto m^{-2.7}, \text{ for } M_{\text{L}} \leq M \leq M_{\text{U}}.$$

This IMF, together with our $f_{7\text{Li}}$ versus mass relation, leads us to an estimate of the average mass, $\bar{m}_{7\text{Li}}$, where ${}^7\text{Li}$ is undepleted for every solar mass of matter processed through Population III stars:

$$\bar{m}_{7\text{Li}} = \frac{\int_{M_{\text{L}}}^{M_{\text{U}}} f_{7\text{Li}} m^{-1.7} dm}{\int_{M_{\text{L}}}^{M_{\text{U}}} m^{-1.7} dm} \quad (3)$$

Considering a lower- and upper-mass range of $M_{\text{L}} = 1 M_{\odot}$ and $M_{\text{U}} = 40 M_{\odot}$, respectively, equation 3 leads to an average $\bar{m}_{7\text{Li}} = 6.9 \times 10^{-3} M_{\odot}$. We believe that our adopted upper mass cut is well justified. Very massive stars ($M_{\star} > 100 M_{\odot}$) in the first generation have been suggested (Oh et al. 2001). The presence of such massive stars is not, however, supported by the observed compositions of very and extremely metal-poor stars (lack of an observed odd-even pattern), nor are they required for reionization of the intergalactic medium (Tumlinson, Venkatesan, & Shull 2004). HE 1327-2326 and HE 0107-5240 ($[\text{Fe}/\text{H}] = -5.4$; Christlieb et al. 2002) are both carbon-rich stars, while HE 1327-2326 is also barium rich. Recent models of very massive stars, however, yield no significant carbon or r-process elements (Heger & Woosley 2002). Contrary to our M_{U} , which we believe is plausible, a higher M_{L} around 10 M_{\odot} is more likely, because of the absence of efficient coolants of the ISM, such as C and O at very low or zero metallicity (Bromm & Loeb 2003). If we

³All of our models above 6 M_{\odot} are still contracting when they reach a central temperature of 10^8 K. Due to the absence of CNO, and the lower efficiency of proton-proton chains in these temperature regimes, these Population III models contract until they ignite the triple- α reaction, which subsequently allows the CNO cycle to begin (Ezer & Cameron 1971).

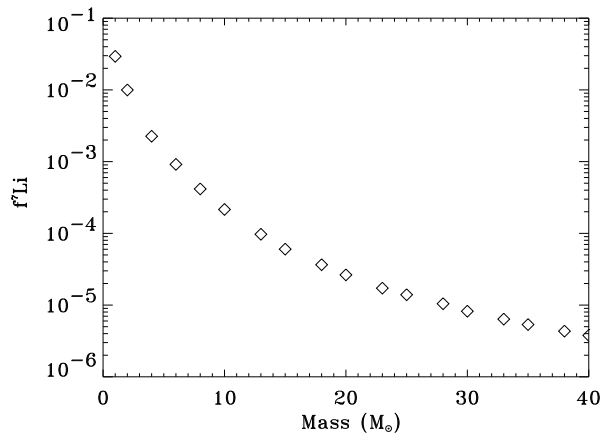


Fig. 4.— Fraction of the mass, f_{Li} , in the outer layers, where ${}^7\text{Li}$ is not depleted in Population III objects, as a function of the total mass.

take $M_{\text{I}} = 10 M_{\odot}$ and $M_{\text{II}} = 40 M_{\odot}$, we evaluate $\bar{m}_{\text{Li}} = 6.7 \times 10^{-5} M_{\odot}$ from equation 3. In either case ($M_{\text{L}} = 1 M_{\odot}$ or $M_{\text{L}} = 10 M_{\odot}$), only a very small fraction of the astrated material is not depleted in lithium.

How does \bar{m}_{Li} relate to the amount of ${}^7\text{Li}$ left behind by the first generation of stars? One could argue that stellar evolution is able to produce ${}^7\text{Li}$, so that our \bar{m}_{Li} could be a lower limit. However, it is presently difficult for suggested early lithium production processes to produce an amount of ${}^7\text{Li}$ at a level of ~ 2 . Out of the three processes that are usually invoked for lithium production by stars, two are related to intermediate- or low-mass stars, the hot bottom burning process in red/Asymptotic Giant-Branch (AGB) stars (Sackmann & Boothroyd 1992; Sackmann & Boothroyd 1999), and novae explosions (Hernanz et al. 1996). The low-mass objects are responsible for the transition in the typical chemical compositions from halo to disk stars. This occurs in a metallicity regime much higher than the one we are dealing with here. The (massive) AGB stars could affect Galactic chemical history earlier, because they have evolutionary timescales as short as 40 Myr. But the present Galactic chemical evolution models suggest that AGB stars have a negligible impact on ${}^7\text{Li}$ history before a metallicity $[\text{Fe}/\text{H}] = -0.5$ is reached (Romano et al. 2001). If they

were to contribute significantly to early ${}^7\text{Li}$ history, it would require the ad-hoc hypothesis that very strong mass loss (“super winds”) occurs precisely at the moment when the surface of the star is lithium rich (Ventura, D’Antona, & Mazzitelli 2002). The low efficiency of AGB stars as lithium factories is also supported observationally. North (1995) notices that the barium-rich stars whose abundance patterns are explained by mass transfer from an AGB companion are also lithium poor ($A({}^7\text{Li}) \leq 1.8$ in most cases). Finally the characteristic s-process pattern appears in halo stars once $[\text{Fe}/\text{H}] \geq -2.6$ (Truran et al. 2002, Simmerer et al. 2004, and references therein). This suggests that AGB stars, the main sites for s-process nucleosynthesis, do not start to affect the Galactic composition until a metallicity is achieved which corresponds to objects on the Spite Plateau. If, despite these clues, we still consider that the intermediate-mass stars could affect early lithium history we must remember that in Λ -CDM cosmology the halo of the Galaxy is thought to have formed from cannibalization of smaller dwarf galaxies or an early generation of globular clusters. For a 100 pc to 1 kpc sized dwarf galaxy, the ISM should be rather well-mixed in a short amount of time, certainly less than 40 Myr (see §5). Therefore, no ${}^7\text{Li}$ inhomogeneities are expected because of the action of the first intermediate-mass stars. The third mechanism that could be invoked for ${}^7\text{Li}$ production is the supernova ν -process. It is associated with neutrino-wind induced reactions during core-collapse supernovae (hereafter SNe). The Timmes et al. (1995) chemical-evolution models suggest that the amount of ${}^7\text{Li}$ produced by this process is negligible in comparison to $A({}^7\text{Li}) \sim 2$ at metallicities below $[\text{Fe}/\text{H}] = -1.0$. We hasten to add, however, that we have been made aware of some recent computations of zero-metallicity core-collapse SNe that result in higher lithium production than previously thought (A. Heger, private communication). Hence, it may be premature to conclude that lithium production cannot have had an early impact.

Bearing the above in mind, we neglected ${}^7\text{Li}$ production processes in our discussion. Furthermore, we note that if these processes were to affect the early Galactic history of ${}^7\text{Li}$ one would expect significant variations in the observed ${}^7\text{Li}$ abundance at metallicities lower than the transi-

tion between Population II (where $A(^7\text{Li}) \sim 2.1$) and the young Population I low-mass stars (where $A(^7\text{Li}) \sim 3.2$). Indeed, even our value of $\bar{m}_{^7\text{Li}}$ is probably an upper limit. First, the stars in the range from 40 to 100 M_\odot will presumably lower $\bar{m}_{^7\text{Li}}$ further, as the trend of $m_{^7\text{Li}}$ with mass in Figure 4 already suggests. Secondly, rotationally-induced mixing could bring the surface matter down into regions of the star where lithium encounters proton capture.

The effects of rotation have just begun to be investigated in models of Population III stars (Hirschi et al. 2006, Hirschi et al. 2006; Meynet, Ekström, & Maeder 2006). We draw attention to those models in which the authors have followed the evolution of $[\text{Fe}/\text{H}] < -6$ massive (20-85 M_\odot), rapidly rotating (300-800 km s^{-1}) stars over their relatively short (several Myr) lifetimes. The most massive of these models ($M_{\text{star}} > 40M_\odot$) experience strong mass loss when they become red supergiants. They are shown to have enriched surfaces in primary C, N and O (nitrogen is a species whose production requires temperatures well above 2.5×10^6 K, hence it goes along with lithium depletion). The net effect of internal rotationally-induced mixing and mass loss is to inject prodigious amounts of C, N, and O into the early ISM. This can raise the level of total metallicity to above the critical value for low-mass star formation to occur. The stars formed from these material will thus reflect the peculiar composition of these ejecta (see §6). We will return to an examination of the possibility of rotationally-induced mixing for explaining the unique composition patterns of HE 1327-2326 and HE 0107-5240, but first we focus on the consequences of a low $\bar{m}_{^7\text{Li}}$ for Population III stars.

If we consider the predictions from the models for ^7Li around the main-sequence-turnoff for halo stars, we find that these objects have depleted roughly 0.2 dex of their initial ^7Li , mostly due to microscopic diffusion and gravitational settling, as the non-standard turbulent-mixing near BCZ can be considered as a secondary effect (Richard et al. 2005; Piau 2006). Since the MS-turnoff Spite Plateau stars with metallicities $[\text{Fe}/\text{H}] \sim -3$ now exhibit $A(^7\text{Li})=2.1$ to 2.2^4 , this means that their

lithium abundances at the time of their formation was nearly $A(^7\text{Li}) = 2.3$ to 2.4 . In turn, we can posit that this lithium abundance is that which has resulted after mixing of Population III processed ejecta with the BBN-composition ISM. If we take the BBN lithium abundance to be $A(^7\text{Li}) = 2.6$, we conclude that Population III stars are responsible for a depletion on the order of $\Delta^7\text{Li} = 0.2$ to 0.3 dex in the very early epochs of the Galaxy. As we have shown that Population III objects fully destroy their initial lithium, $\Delta^7\text{Li}$ directly translates into the fraction of gas mass that was originally astrated by Population III stars. Indeed, it suggests that between a third and a half of the baryonic mass of the halo of the Galaxy was originally processed through Population III objects. More generally, we can relate the fraction of mass x_{PopIII} astrated by population III to $\Delta^7\text{Li}$:

$$x_{\text{PopIII}} = \frac{1 - 10^{-\Delta^7\text{Li}}}{1 - \bar{m}_{^7\text{Li}}} \sim 1 - 10^{-\Delta^7\text{Li}} \quad (4)$$

Equation 4 is interesting, in the sense that it relates observed and predicted quantities to the presently poorly-known efficiency of the Galaxy to form its first generation of stars. The quantity $\Delta^7\text{Li}$ depends on BBN, but is also closely related to our understanding of the internal dynamics of low-mass Population II stars and their measured surface abundances, while $\bar{m}_{^7\text{Li}}$ is set by the structure of zero-metallicity stars and the IMF in the early halo of the Galaxy. If we set $\bar{m}_{^7\text{Li}} = 6.7 \times 10^{-5}$ and $\Delta^7\text{Li} = 0.3$ in equation 4, we obtain $x_{\text{PopIII}} \sim 0.50$. If, at the other extreme, we set $\bar{m}_{^7\text{Li}} = 6.9 \times 10^{-3}$ and $\Delta^7\text{Li} = 0.2$ in equation 4, we obtain $x_{\text{PopIII}} \sim 0.37$. The levels of astration we predict are quite important and should in turn have consequences on (1) the early nucleosynthesis in the Galaxy, (2) the injection of cosmic rays and subsequent light elements production in the ISM when the (massive) Population III stars end their lives, and (3) the possible reionization of the early interstellar/intergalactic medium. Although not the main focus of the article, these three points are of cosmological significance, and deserve some comments, as given below.

(Ryan et al. 1999), while others suggest $A(^7\text{Li}) \sim 2.2$ (Bonifacio et al. 2006). The observations of the latter authors also suggest the presence of turn-off halo stars that exhibit $A(^7\text{Li}) < 2$, as is discussed in §2.

⁴There is still a debate about the exact value of the Spite Plateau at $[\text{Fe}/\text{H}] \sim -3$. Some authors claim $A(^7\text{Li}) \sim 2.1$

(1) Stellar nucleosynthesis. We predict that between a third and a half of the matter constituting the present halo stars was astrated by Population III stars. This large fraction seems worrying at first sight because it predicts a large amount of early metal production. Some authors (Ricotti & Ostriker 2004) have argued that the enrichment in metals of the intergalactic medium (hereafter IGM) by Population III stars constrains their masses or numbers. However, our computations only imply that only up to half of the mass of the present Population II stars was processed by Population III progenitors. This is much smaller than the mass in the Galactic disk, and should not be confused with it (see below). The SNe that take place at the end of the lives of massive Population III stars may have occurred at much lower masses than these stars possessed originally, due to the effect of possibly large amounts of mass loss from Population III massive stars during their lifetimes. Recent studies show that they tend to reach their break-up velocities during the MS because of their greater compactness, and their lower initial angular momentum loss through magnetic winds than their Population I counterparts. Furthermore, rotationally-induced mixing may, in the course of their evolution, bring metals to the surface, which subsequently triggers stronger mass loss through stellar winds (Hirschi et al. 2006; Meynet et al. 2006). Contrary to previous assumptions, massive Population III stars would thereby lose a significant amount of mass before exploding. The mass actually involved in the advanced stages of quiescent or explosive burning would be much smaller than the ZAMS mass. Thus, from the point of view of metal enrichment, the mass astrated by Population III stars is smaller than half of the halo mass. It is finally noteworthy that the wind composition in models of massive stars having $[\text{Fe}/\text{H}] = -6.6$ (Hirschi 2006) fits well the CNO abundance ratios observed in HE 1327-2326 or HE 0107-5240, which are very different from the yields of massive SNe, which exhibit much more oxygen than nitrogen or carbon (Hirschi et al. 2006; Chieffi & Limongi 2004). This suggests that the metals are less efficiently ejected from the first SNe than they are from the following generations.

Another possible issue raised by the hypothesized astration in Population III is that, wherever

^7Li is depleted, ^2H is also depleted. We therefore predict that between a third and a half of the primordial deuterium is already depleted in the Population II stars. The primordial deuterium-to-hydrogen ratio expected from WMAP constraints is 2.60×10^{-5} (Coc et al. 2004), which is also in good agreement with the measurements along the lines of sight to distant quasars, $(^2\text{H}/\text{H})_{\text{p}} \sim 3 \times 10^{-5}$ (O’Meara et al. 2001; Burles 2002, and references therein). On the other hand, the present deuterium-to-hydrogen ratio in the local ISM lies around 1.5×10^{-5} (Linsky 1998; Oliveira et al. 2003), while the pre-solar ratio determined from the solar wind or the spectra of gas-giant planets is between 2×10^{-5} and 6×10^{-5} (see Lemoine et al. 1999 for references). Knowing that deuterium is only destroyed by successive generations of stars, both the $^2\text{H}/^1\text{H}$ ratios of the pre-solar medium⁵ and the present local ISM should be smaller than 1.7×10^{-5} (1.5×10^{-5}) if one third (respectively one half) of the matter of the Galaxy has been astrated by Population III objects. However, the paradigm we suggest is that only Population II objects result from a mix of Population III ejecta (and winds) with genuinely BBN composition matter. This does not imply the same is true for Population I objects. The infall of ^2H -rich intergalactic matter of (near) BBN composition onto the young Galactic disk may solve this apparent deuterium discrepancy, provided it occurs after the formation of the Population II stars and during the formation of the successive generation of Population I stars. Such an infall scenario is indeed supported by the modeling of the deuterium history in the Galaxy (Lubowich et al. 2000; Romano et al. 2006). Furthermore, the stellar mass of the Galactic halo is $\sim 2 \times 10^9 M_{\odot}$ (Bullock & Johnston 2005), i.e., only a few percent of the total Galactic mass. We mention finally that the observed deuterium abundances in the present ISM exhibit a large amount of scatter, which suggests a quite complex history for this species. Accurate measurements remain a matter of debate (Lemoine et al. 1999; Romano et al. 2006).

(2) ISM nucleosynthesis. Since the seminal works of Reeves, Fowler, & Hoyle (1970) and Meneguzzi, Audouze, & Reeves (1971), it has been

⁵The high $^2\text{H}/^1\text{H}$ ratio in the pre-solar medium deuterium is problematic if the Galaxy evolves as a chemically isolated system.

known that spallation and non-thermal fusion processes induced by cosmic-ray interactions with the ISM can explain some of the observational patterns of the light elements, namely Li, Be, and B over the history of the Galaxy. A discussion of this topic is beyond the scope of the present work; for recent developments about the LiBeB Galactic evolution through spallation we direct the reader to Lemoine, Vangioni-Flam, & Cassé (1998) and Fields & Olive (1999). However, we wish to make some brief remarks about the implications of our hypothesis of a significant early astration for the ${}^6\text{Li}$ isotope.

Although ${}^6\text{Li}$ has been detected for some time in halo turnoff stars (Cayrel et al. 1999; Nissen et al. 1999), the sample of objects with claimed detections has recently been increased significantly (Inoue et al. 2005; Asplund et al. 2006). The observations of these authors suggest $A({}^6\text{Li}) \sim 1$ is constant for metallicities in the range $-2.7 \leq [\text{Fe}/\text{H}] \leq -0.6$. Such a ${}^6\text{Li}$ plateau is puzzling because, contrary to ${}^7\text{Li}$, the amount of ${}^6\text{Li}$ produced by BBN should be negligible (Vangioni-Flam et al. 1999; see Jedamzik 2004 for a possible non-standard ${}^6\text{Li}$ BBN scenario). However, the presence of a ${}^6\text{Li}$ plateau over such a broad range in metallicity suggests a pre-Galactic origin. Making no assumptions on the mechanism(s) accelerating the particles in the early ISM, Rollinde, Vangioni, & Olive (2005) showed that a burst of cosmological cosmic rays could explain the ${}^6\text{Li}$ observed at very low metallicity without overproducing ${}^7\text{Li}$. But what phenomenon produces the energy required for fusion or spallation in the ISM? One mechanism that has been proposed for accelerating the nuclei is related to the shocks associated with structure formation (Suzuki & Inoue 2002). This process was, however, recently criticized by Prantzos (2006) because it produces too little energy, and would lead to an increase of ${}^6\text{Li}$ during a large fraction of the early Galactic history, rather than to a plateau. Population III supernovae are alternate candidates for ${}^6\text{Li}$ production. They can inject the energy required for the $\alpha + \alpha$ fusion reactions thought to be the main channel of ${}^6\text{Li}$ production in the very metal-poor early ISM. In this respect, the large fraction of material astrated by massive Population III stars we predict here is interesting, because it supports a large number of early supernovae events. As previously noted by

Prantzos (2006), the extension of the ${}^6\text{Li}$ plateau down to very low metallicities places constraints on the nature of the early SNe, if they are responsible for its production. In the case of the present-day composition supernovae the ratio of kinetic energy (required to induce enough ${}^6\text{Li}$ production) to the iron injection in the ISM is such that Prantzos (2006) establishes that it is not possible to produce $A({}^6\text{Li}) \sim 1$ below $[\text{Fe}/\text{H}] = -1.4$. However, the yields of Population III supernovae could differ from those at present. As stressed by the same author (Prantzos 2005), the electron mole fraction, the mass cut, and (above all) the rotationally-induced effects have to be taken into account carefully before and during the explosion. The uncertainties on these parameters leave Population III supernovae as potential candidates for ${}^6\text{Li}$ production at very low metallicity. Clearly, this possibility should be explored more thoroughly in future works.

(3) Reionization. The reionization of the Universe can be tracked because it affects the optical depth to the cosmic microwave background (Spergel et al. 2003). It is thought to have occurred between a redshift of $z = 20$ and $z = 6$ (Venkatesan 2006, and references therein); massive Population III stars are strong candidates as the contributors of this ionizing radiation. If reionization is related to the first stars, it is also necessarily connected to Galactic chemical history. For instance, carbon and oxygen are observed in the IGM and, provided the IMF and the chemical yields of Population III stars are known, it is possible to constrain the reionization induced by the first stars (Venkatesan & Truran 2003). In our approach, ${}^7\text{Li}$ also provides crucial information about the efficiency of the first stars to convert baryonic matter into IGM-ionizing photons, because it suggests that between one third and one half of the baryonic matter of the halo ($\sim 10^9 M_\odot$) was processed in the first stars. Indeed, ${}^7\text{Li}$ might be a more reliable probe than other species because of its simpler evolution; it is systematically destroyed in the astration process in a way that depends weakly on the IMF (see above). On the contrary, the production of CNO and the other heavy elements probably depends on the IMF, on the late stages of stellar evolution, and on the complex and still to be fully investigated rotationally-induced mixing effects (Hirshi et al. 2006a, 2006b).

4. The Low Metallicity End of the Spite Plateau ?

As noted in §2 above, several observed facts about the nature of the Spite Plateau are of central importance to testing our Li-astration model. First, the star-to-star scatter in measured $A(^7\text{Li})$ for metal-poor stars on the plateau is *extremely* small, on the order of 0.03-0.05 dex (Ryan et al. 1999; Asplund et al. 2006; Bonifacio et al. 2006), well within the expected observational errors. Secondly, at the lowest metallicity end of the plateau, $[\text{Fe}/\text{H}] < -2.5$, there appears to be evidence for either a downturn in the ^7Li abundance relative to the more metal-rich stars ($-2.5 \leq [\text{Fe}/\text{H}] \leq -1.5$), or else an increase in the level of star-to-star scatter (Bonifacio et al. 2006). This second point is dependent on observations of only a handful of stars, and hence needs to be explored with much larger samples in the near future.

In our Li-astration model the downward trend (or increased scatter) of ^7Li abundances is interpreted as the imprint of the mixing between the Population III ejecta and the ISM of BBN composition. We discuss the turbulent mixing of the early Galaxy in the next section. Before the low-metallicity edge of the plateau at $[\text{Fe}/\text{H}] \sim -2.5$, not enough metals have been mixed into the pure BBN-composition ISM and the low-mass stars form more efficiently in the unmixed ejecta because they contain the required amount of coolants, primarily C and O. This stage extends from $[\text{Fe}/\text{H}] = -3.5$, which could be the lower metallicity limit for low-mass star formation (Bromm & Loeb 2003) up to $[\text{Fe}/\text{H}] = -2.5$. The increase of scatter in r-process elements (Truran et al. 2002) favors this hypothesis of still inhomogeneous ISM for metallicities lower than $[\text{Fe}/\text{H}] \sim -2.5$. However, we note that the scatter associated with r-process elements lingers in the higher-metallicity regime at least up to $[\text{Fe}/\text{H}] = -2$. For metallicities in the range $[\text{Fe}/\text{H}] \sim -5$ to ~ -3.5 , it has been very recently suggested by Karlsson (2006) that the turbulence induced by the SNe explosions and the ionizing effects of the massive first stars could lower the rate of star formation. This would explain the apparent absence of stars on this metallicity range. Interestingly, Karlsson interprets HE 1327-2326 the same way as we do, as a hyper metal-poor star that formed predominantly out of the CNO-enriched

ejecta of a massive zero-metallicity star of the first generation. We stress that this interpretation is in agreement with the yields of Population III models including rotation mixing as mentioned by Hirschi et al. (2006) (see §6). In this case HE 1327-2326 would be lithium poor for the same reason that it is CNO rich – because of astration of most of its mass by one (or a few) massive Population III progenitor(s).

5. Turbulent Mixing in the Early Galaxy

Observations of low-mass star formation in our Galaxy suggest that such stars form predominantly in giant molecular clouds on time scales from 0.1 to ~ 1 Myr (Ward-Thompson, Motte, & André 1999). Observations of these molecular clouds (Lis et al. 1996; Miesch, Scalo, & Bally 1999) have also shown that the gas within them is very turbulent. Similarly, observations of starburst systems, such as M82 (Pedlar, Muxlow, & Wills 2003), suggest that star formation can take place in strongly shocked, turbulent environments with very high rates of energy input from massive stars. In the case of early-epoch galaxies there are also both theoretical and observational arguments to support a similar connection between turbulence and star formation. We stress, however, that the low-mass star formation in the present Galaxy cannot be transposed without caution to the extremely metal-poor proto-Galactic ISM (Bromm & Loeb 2003). From the modeling point of view, Elmegreen (1994) and Salvaterra, Ferrara, & Schneider (2004) suggested that converging shocks in a proto-Galactic medium with high rates of supernova explosions might be one possible mechanism for forming low-mass stars. From the observational point of view the ULIRGs provide support for proto-Galactic ISMs that are strongly influenced by massive stars and their ejecta. Therefore, in this section, we take such a SN-driven proto-Galactic ISM as our working paradigm, and explore metallicity evolution, lithium depletion, and low-mass star formation within this context. Metal-poor stars, and in particular, hyper metal-poor stars, provide essential clues about this early Galactic history.

It is beyond the scope of our present understanding to have a complete theory for low- and high-mass star formation in our Galaxy. Nev-

ertheless, some insights may well be obtained. For example, if turbulence in the ISM is strong, and mixing is extremely efficient over very short timescales, then it is reasonable to expect that alpha-capture elements (which are made in all Type II SNe) should be well-mixed into the proto-Galactic environment. Furthermore, if the timescales required for complete mixing are comparable to the timescales for low-mass star formation, then each generation of low-mass stars in the halo, as cataloged by a specific value of $[\text{Fe}/\text{H}]$, should also exhibit a small scatter in the alpha-capture elements (see §6). On the other hand, it is also possible that the earliest SNe were of the much rarer pair-instability type (Salvaterra et al. 2004) and, as a result, the earliest ISMs were not strongly turbulent. In that case we would expect hyper metal-poor low-mass stars to form only in the high-metallicity ejecta left behind by such SNe. Then, the scatter expected in metals in hyper metal-poor stars would be large, because they would have formed in response to individual events, not all of which are identical.

If the primordial SNe were plentiful and evenly distributed we would expect the proto-Galactic ISM to be strongly turbulent. In such a situation, the ejecta from the posited Population III stars can be efficiently mixed with primordial gas, resulting in a net dilution of the amount of ${}^7\text{Li}$ in the natal gas clouds that formed the next generation of stars (including low-mass stars). Theoretical studies of turbulent mixing have been carried out by Bateman & Larson (1993), Roy & Kunth (1995), and Oey (2003). The problem has also been studied numerically by Klessen & Lin (2003) and Balsara & Kim (2005). The latter authors were specifically interested in SN-driven turbulence, the very process that interests us here. They found that for SN-driven turbulence that involves a supernova rate that is eight times the present Galactic rate, the turbulent diffusion coefficient is given by $\eta_{\text{turb}} = 5.7 \times 10^{26} \text{cm}^2/\text{sec}$. Since this is a diffusive process, the diffusion scales directly as the square of the length of the system and inversely as the diffusion coefficient. Therefore, we consider a 100 pc region, which could either be a proto-globular cluster system or a part of a larger system, like M82, that is undergoing an episode of vigorous star formation and SNe explosions. Taking L_{100} to be a length measured in 100 pc and $\tau_{\text{diff},6}$ to be

the diffusion time, measured in millions of years, we obtain $\tau_{\text{diff},6} = 5.3 L_{100}^2 \text{Myr}$. This timescale is comparable to the total lifetime of a massive star, with the consequence that each generation of stars that form do so in an environment where the metals from the previous generation are turbulently mixed in.

It is also important to realize that turbulence only mixes the metals at a macroscopic level. An enhanced metallicity also produces an enhanced cooling rate, thus playing an important role in regulating star formation. Since metals play an important role in setting the cooling rate of gas, it is important to mix the metals down to the molecular level. If such mixing is achieved for a particular element, one would expect that element to show a very small scatter with increasing $[\text{Fe}/\text{H}]$. The question of mixing the metals down to the molecular level has been looked at theoretically by Oey (2003) and computationally by Balsara & Kim (2005). The latter authors found that such mixing occurs unusually fast in turbulent environments. For example, in the case of the ISM discussed above, they found that mixing of metals down to the molecular level took place in a fraction of a million years. The implication is that, if turbulent eddies can efficiently mix the metals on the large eddy-bearing scales, thus conveying supernova ejecta from one location to another, then the ejecta will be mixed down to the molecular level in a time that is even shorter than the bulk turbulent diffusion time. As a result, we anticipate that metals that are produced in SNe of all mass ranges will be well mixed. The production of scatter in the metals is a consequence of certain mass ranges of progenitor stars producing certain species with above-average abundance, as well as local pollution events (e.g., low-mass star formation in the near vicinity of a given SNe, or mass-transfer events at later times).

The implication of the above discussion for ${}^7\text{Li}$ is as follows. We see from Figure 2 that dwarfs with $[\text{Fe}/\text{H}] > -2.5$ exhibit an extremely small scatter in $A({}^7\text{Li})$. A high rate of early turbulent mixing is indeed the most natural way of explaining this low scatter. To obtain such a high rate of turbulent mixing one requires a high rate of SNe, which is *a-posteriori* justified if ~ 30 to $\sim 50\%$ of the primordial matter of the halo was processed by massive stars by the time $[\text{Fe}/\text{H}]$ reached ~ -2.5

(§3). Massive Population III stars not only explain the lowered mean value of $A(^7\text{Li})$ from the BBN value, because they deplete ^7Li , but they also explain the small scatter *above* $[\text{Fe}/\text{H}] \sim -2.5$ resulting from a very high SNe rate and the subsequent vigorous ISM mixing at that epoch.

The perspective we have now developed would also enable us to understand the trends in Figure 2 for $[\text{Fe}/\text{H}] < -2.5$, where the scatter in $A(^7\text{Li})$ slightly increases with decreasing $[\text{Fe}/\text{H}]$. If the scatter keeps increasing with decreasing $[\text{Fe}/\text{H}]$, as more HE 1327-2326-like dwarfs are found, it would imply that the hyper metal-poor dwarfs formed from mixtures of various proportions between the metal-enhanced ejecta of Population III progenitors and the BBN-composition ISM. It could also imply that these stars and the hyper metal-poor dwarfs formed in response to individual supernova events, before a sufficient number or rate of such supernova events could have produced substantial amounts of turbulence in the proto-Galactic ISM. As mentioned before, the scatter in r-process elements starting at $[\text{Fe}/\text{H}] \sim -2$ and gradually increasing below ~ -2.5 indeed favors this possibility. If, on the other hand, stars with $[\text{Fe}/\text{H}] < -2.5$ show a small scatter in ^7Li , it would imply that the ISM and SNe ejecta are efficiently mixed before these stars form. Finally, if other hyper metal-poor stars such as HE 1327-2326 are found to exhibit a complete absence of ^7Li , it would imply that such stars cannot form anywhere but within the ejecta of earlier massive stars.

6. Additional Consequences of the Population III Processing model

In §3 we have drawn attention above to the recent models of Hirschi (2006), Hirschi et al. (2006), and Meynet, Ekström, & Maeder (2006), in which they have followed the evolution of $[\text{Fe}/\text{H}] < -6$ massive ($20\text{--}85 M_\odot$), rapidly rotating ($300\text{--}800 \text{ km s}^{-1}$) stars. Such models experience rotationally-induced mixing, which affects their nucleosynthesis and, in the most massive ones ($M_\star > 40 M_\odot$), triggers strong mass loss. Eventually, prodigious amounts of C, N, and O are ejected into the ISM due to mass loss or subsequent SNe explosions. This material will be barren of primordial Li, but, as pointed by Hirschi et al. (2006), enriched in CNO to a level that could allow low-

mass star formation (Bromm & Loeb 2003).

There are a number of other expectations for the stellar surface compositions of the next-generation stars if rapidly-rotating zero-metallicity stars are appealed to as the site of the Population III processing which we invoke for lithium destruction. We discuss these in turn below.

6.1. Unique Abundance Patterns Among Stars of the Lowest Metallicity

The two known hyper metal-poor stars, HE 0107-5240 (Christlieb et al. 2002, 2004a), and HE 1327-2326 (Frebel et al. 2005; Aoki et al. 2006a), both with $[\text{Fe}/\text{H}] < -5.0$, exhibit similar elemental abundance patterns, featuring enormous overabundances (relative to Fe) of C, N, O, and (at least in the case of HE 1327-2326), of the elements Na, Mg, and Al. Both of these stars, as well as the two stars CS 22949-037 (Depagne et al. 2002) and CS 29498-043 (Aoki et al. 2002, 2004), with $[\text{Fe}/\text{H}] = -4.0$ (Cayrel et al. 2004) and $[\text{Fe}/\text{H}] = -3.5$ (Aoki et al. 2004), respectively, are classified as Carbon-Enhanced Metal-Poor (CEMP) stars, according to the suggested taxonomy of Beers & Christlieb (2005). All four are further sub-classified as CEMP-no stars, as none of them exhibit the presence of Ba (note that only an upper limit, $[\text{Ba}/\text{Fe}] < 1.7$, exists for HE 1327-2326). These broadly similar abundance patterns are thus far not seen *in any other stars* with $[\text{Fe}/\text{H}] > -3.5$. Furthermore, Aoki et al. (2003) and Aoki et al. (2006b) suggest that no more than 20% of all CEMP stars should be classified as CEMP-no stars, the remainder being of the class that exhibit strong s-process (classified as CEMP-s) or r/s-process (classified as CEMP-r/s) elemental abundance signatures.

Predicted elemental abundance patterns that bear a strong similarity to the stars discussed above are obtained in the “wind only” models described by Meynet et al. (2006, their Figure 8; Hirschi 2006; Hirschi et al. 2006). In the view of our present scenario, these four stars may well have recorded a nearly unaltered picture of the material that was produced by their massive Population III zero-metallicity progenitors.

6.2. Production of Primary Nitrogen and the Observed Trends of [N/O] and [C/O] at Low Metallicity

Spite et al. (2005) have discussed the behavior of, in particular, nitrogen, among the stars from the Cayrel et al. (2004) sample that are not expected to have altered their surface values of CNO during their lifetimes (the “unmixed stars” in the Spite et al. sample). They concluded that it was likely that some source of primary nitrogen (that is, N that is formed directly from He, rather than requiring conversion associated with CN processing) was necessary to explain the observed high [N/O] (and [C/O]) ratios at low metallicity. Chiappini, Matteucci, & Ballero (2005) and, very recently, Chiappini et al. (2006, based on the new yields computed by Meynet et al. 2006 and Hirschi et al. 2006 for rapidly rotating zero-metallicity massive stars) concluded that such behaviors might be expected to follow if the Population III processing scenario we consider in the context of ${}^7\text{Li}$ astration applies in the early Galaxy. In particular, the agreement of the new chemical evolution models from Chiappini et al. (2006) with observations of the [N/O] and [C/O] trends at low metallicity is quite striking. We recall here (see §3) that these ratios do not correspond at all to those expected from typical Type II SNe ejecta.

6.3. The Lack of Scatter in Alpha- and Iron-Peak Elements at Low Metallicity

One of the clear outcomes of recent high-S/N, high-resolution investigations of very metal-poor stars (e.g., Carretta et al. 2002; Cayrel et al. 2004; Arnone et al. 2005) is the finding that an extremely small star-to-star scatter in the observed alpha- and iron-peak elements exists for most stars with $[\text{Fe}/\text{H}] < -2.0$. The implications of this result have been discussed by many authors. It is difficult to imagine that, if Type II SNe with a wide range of initial masses are responsible for the production of these elements, that there should be such a small observed scatter. It seems, rather, that extremely efficient mixing, of the sort we imagine (see §5) to explain the level of the ${}^7\text{Li}$ Plateau, must have occurred in the ISM for at least the stars with $[\text{Fe}/\text{H}] > -2.5$.

One might wonder about the observed (real)

large star-to-star scatter in the neutron-capture elements. In the view of our present investigation, these would have to be accounted for by “local” pollution, either from binary companions, e.g., AGB stars in the case of s-process-rich metal-poor stars, or the formation of r-process-enhanced stars in the near vicinity of the objects responsible for the production of the r-process elements.

6.4. Carbon at Low Metallicity

The Population III astration model, to which we appeal for lithium depletion, is also a very attractive candidate for at least three carbon-related features of very metal-poor stars with $[\text{Fe}/\text{H}] < -2.0$:

(i) One of the (at first) surprising results of the large modern surveys for metal-poor stars is the apparent large increase in the fraction of carbon-enhanced stars at low metallicity. Although there remains some debate about the precise fraction of CEMP stars with $[\text{Fe}/\text{H}] < -2.0$, recent results from analysis of high-resolution spectra from the HERES survey (Christlieb et al. 2004b; Barklem et al. 2005) by Lucatello et al. (2006) make it clear that at least 20% of all stars at this low metallicity are enhanced in their [C/Fe] ratios by a factor of ten or more above the solar value. Although the sample size is presently small, Beers & Christlieb (2005) point out that 5 of the 12 stars known with $[\text{Fe}/\text{H}] < -3.5$, based on high-resolution spectroscopic studies, are strongly carbon enhanced, roughly 40%. Below $[\text{Fe}/\text{H}] = -5.0$, the fraction is 100% (2 of 2 stars). It seems required that some metallicity-dependent mechanism for the production of large [C/Fe] ratios must be invoked.

(ii) CEMP-s stars can be readily explained by appealing to the presence of a binary companion that has donated s-process and carbon-rich material to the surviving star that is presently observed, however there is no clear-cut model for the production of carbon in the CEMP-no stars, where neutron-capture elements are not found.

(iii) The isotopic ratio ${}^{12}\text{C}/{}^{13}\text{C}$ in CEMP stars also provides interesting constraints on the chemical history of the early halo. Although the numbers of CEMP-no stars for which ${}^{12}\text{C}/{}^{13}\text{C}$ has been measured thus far is still small, it does appear that the observed isotopic ratio in these stars is lower (${}^{12}\text{C}/{}^{13}\text{C} < 10$) than is typically found

for the CEMP-s stars (Beers et al. 2006; Sivarani et al. 2006).

The Population III processing model provides a natural explanation for these features. In particular, no s-process-enriched material is expected to be produced by the massive Population III stars, and it may well not be a coincidence that the great majority of known CEMP-no stars have not yet exhibited the presence of a binary companion from radial velocity monitoring carried out to date. Furthermore the, “wind only” models of Hirschi et al. (2006) and Meynet et al. (2006) produce very low $^{12}\text{C}/^{13}\text{C}$ in the material they eject prior to explosion; predicted ratios in the ejected material are in the range $^{12}\text{C}/^{13}\text{C} = 4\text{--}5$. These change drastically (in their models) only post explosion, rising by many orders of magnitude. The possible association of low $^{12}\text{C}/^{13}\text{C}$ with low Li is clearly of interest for future investigation, in particular for the CEMP-no stars.

7. Summary and Conclusions

We have addressed a new idea and considered its consequences regarding the evolution of ^7Li from Big Bang abundances to Population II halo star abundances. This idea posits that the early lithium history lithium was indeed significantly affected by astration of the matter *before* the Population II stars were formed. The most compelling candidates for this task are the massive Population III stars which, during their lifetimes, suffered considerable mass loss of essentially Li-free and CNO-enhanced material, and when they exploded, provided additional Li-free and metal-enriched matter to the ISM. In this scenario the Population III ejecta and the ISM matter directly inherited from the BBN are subsequently mixed by turbulence. Once enough metals had been injected, the low-mass Population II stars we observe today began to form.

Our starting point for this scheme was the apparent discrepancy between the high primordial ^7Li abundance inferred from BBN predictions and WMAP, $A(^7\text{Li}) = 2.6$ (Coc et al. 2004), and the existing observations of MS-turnoff Population II halo stars, $A(^7\text{Li}) = 2.1$ to 2.2 (see §2). Until now, this issue was mostly addressed by considering the possible depletion of lithium *inside* the Population II stars. A great number of works and various

processes have been invoked to deplete the surfaces of halo stars from their original lithium abundances (e.g., Montalbán & Schatzman 2000; Pinsonneault et al. 2002; Richard et al. 2005; Piau 2006). It is noticeable, however, that explaining a ~ 0.4 dex discrepancy, together with an extremely small scatter on the lithium plateau (around 0.02 dex following Ryan et al. 1999 or Asplund et al. 2006), is a difficult task for any of these processes. For instance, in a preceding paper, Piau (2006) reached the conclusion that only 0.2 dex of the initial ^7Li was in fact depleted. Similarly, Pinsonneault et al. (2002) estimated the depletion has to be in the 0.1 to 0.2 dex range, if one wants to be compatible with the (almost complete) absence of scatter on the plateau. The recent detection of ^6Li in a great number of plateau stars (Asplund et al. 2006) further suggests that the ^7Li abundance observed there has mostly been affected by diffusion, but not by nuclear destruction. Taking the recent Bonifacio et al. (2006) observations into account raises the suspicion of the existence of a decrease in the ^7Li abundance when the metallicity drops below $[\text{Fe}/\text{H}] = -2.5$. This suggests that the end of the Spite Plateau towards low metallicities has now been reached, at roughly this metallicity. The absence of ^7Li in HE 1327-2326, the most metal-poor star presently known (Frebel et al. 2005), reinforces this suspicion.

We checked the predictions from stellar models of Population II turnoff stars for the evolution of ^7Li , assuming several prescriptions for non-standard mixing and microscopic effects (i.e., microscopic diffusion and gravitational settling; §2). Making the assumption that the present observations of $A(^7\text{Li})$ for turnoff stars are correct, we deduced that the required depletion of lithium due to Population III processing lies roughly between 0.2 and 0.3 dex (see Figure 1 of the §1). This value accounts for the amount of lithium destruction per solar mass astrated on the ZAMS in Population III massive stars (§3). Let us now schematically summarize our view of the temporal sequence of events marking the chemical evolution of the early Galactic halo.

7.1. Population III

We interpret the present ^7Li data in halo stars as follows. The first generation of stars forms, and roughly one third to one half of the baryonic mass

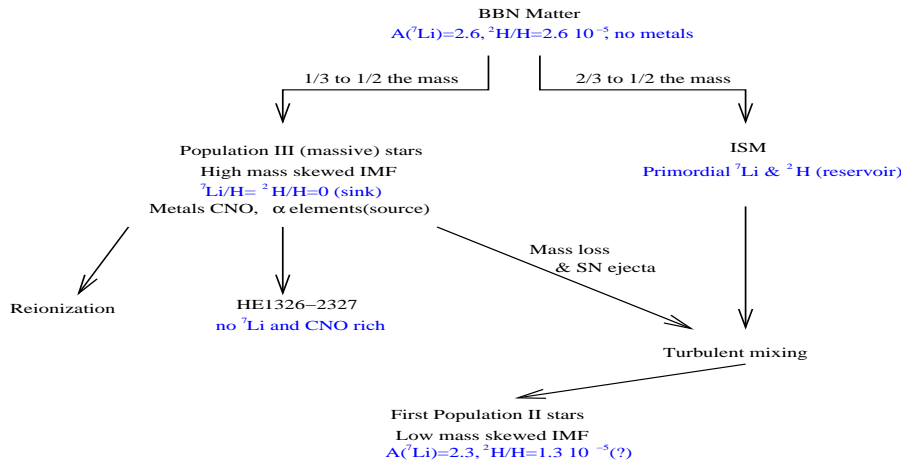


Fig. 5.— Summary of the ${}^7\text{Li}$ and heavier element chemical abundance evolution we suggest at the epoch of the Population III stars. At that time the IMF is probably, contrary to now, skewed towards high-mass stars.

of the halo is processed through them (at least on the ZAMS). The species ${}^7\text{Li}$ and ${}^2\text{H}$ are almost totally destroyed in these first stars. Because of the absence of metals in the early ISM most (all?) of the first stars are massive – the initial IMF probably differs from the present IMF in the sense it is skewed towards larger masses. Therefore, contrary to the present situation, most of the astrated mass then resides in massive objects. These objects presumably lose a large fraction of their mass due to rotational effects (§3), and evolve rapidly into core-collapse supernovae. Globally, this process enriches the early ISM in metals (CNO and α -elements; §6) while it depletes it of light elements (${}^7\text{Li}$ and ${}^2\text{H}$; §3). Figure 5 displays this “genealogy”. The evolution can perhaps be most easily thought of in terms of “sinks”, “sources” and “reservoirs”. Population III stars act as sinks for ${}^7\text{Li}$ and ${}^2\text{H}$, while they act as a sources for the heavy elements. The ISM/IGM, on the other hand, acts as a reservoir for ${}^7\text{Li}$ and ${}^2\text{H}$.

Since they are more metal rich, the winds of the massive Population III stars and the subsequent SNe ejecta that are hardly mixed with the ISM are more prone to form low-mass stars. In this respect, HE 1327-2326 could be one of the objects primarily formed out of the winds and/or SNe ejecta of a Population III star. No ${}^7\text{Li}$ has been detected in its atmosphere, it has a very small $[\text{Fe}/\text{H}]$, but is CNO-rich, as expected from the nucleosynthesis of

early massive objects (Hirschi et al. 2006). In our framework, HE 1327-2326 differs from the typical Population II objects in the sense that it was not formed from a mix of early ISM matter and Population III ejecta. In some respects HE 1327-2326 would be a transition object between Populations III and II. We presented here the first isochrone for objects of the same composition as HE 1327-2326 (§2).

We remark that the relation of Population III yields to the next generation of stars might be a complex issue, and deserves further investigations (§5). For instance, some segregation effects may have occurred in the ejecta, which could have affected the ratio between the different metals (Venkatesan, Nath, & Shull 2006). Furthermore, the shock waves of the first SNe may have triggered low-mass star formation in a medium predominantly made of metal-free matter (Salvaterra et al. 2004). Depending on the amount of mixing, such low-mass Population II stars could simultaneously exhibit lithium lines and extremely low ($[\text{Fe}/\text{H}] < -3$) metallicities. Investigating the $A({}^7\text{Li})$ scatter in halo stars with $[\text{Fe}/\text{H}] < -2.5$ will provide important insights on this question.

7.2. Turbulent Mixing

We have examined the question of turbulent mixing of metal-bearing supernova ejecta in the

proto-Galactic ISM. For high rates of SNe we find that the turbulent diffusion of metals is very efficient. This is especially true in the context of bottom-up, Λ -CDM cosmologies suggested by WMAP. Efficient mixing of metals at and above $[\text{Fe}/\text{H}] \sim -2.5$ is a very economical strategy for explaining the small scatter in $A(^7\text{Li})$ at those metallicities. While the idea was not fully developed here, the small scatter observed in alpha-capture elements by Cayrel et al. (2004) also provides strong support for a scenario based on efficient turbulent mixing.

At values of $[\text{Fe}/\text{H}]$ below -2.5 we expect that we should begin to probe the effects of individual SNe, i.e., an insufficient sufficient number of SNe have gone off in order to drive the turbulent mixing of the proto-Galactic ISM. In those extremely early epochs we should expect to see the scatter in $A(^7\text{Li})$ increase with decreasing metallicity, provided ^7Li is detected. Some of the limited available data does exhibit this behavior, but better statistics are required. Finally, we arrive at the interesting possibility that the ages of the hyper metal-poor stars (if they could be readily measured) would provide an alternative indication of the epoch of reionization. Our results also have far-reaching consequences for cosmological simulations, because they imply that turbulent processes may have been important at early epochs.

7.3. Population II

As the turbulence in the Galactic medium mixes ever more Population III SNe ejecta into the BBN-composition matter, the IMF becomes closer to what it is today. Indeed, it is predicted that above a critical metallicity (around $Z = 10^{-4}Z_{\odot}$, following Bromm & Loeb 2003) low-mass stars begin to form. Interestingly, the heavy-element mass fraction and $[\text{O}/\text{H}]$ ratio we compute for HE 1327-2326 are $Z = 3.1 \times 10^{-4}$ and -1.8 , respectively, which is comparable to the standard Spite Plateau composition where $Z = 3.0 \times 10^{-4}$, while $[\text{O}/\text{H}] = -1.7$ and $[\text{Fe}/\text{H}] = -2$. The change in the IMF is a crucial point for the subsequent evolution of the baryonic matter in the halo – by the time the low-mass stars gather most of the astrated matter, massive stars no longer act as a significant sink for ^7Li or ^2H . On the main sequence, the massive or intermediate-mass Population II stars deplete the light elements very efficiently, as do their Popu-

lation III counterparts. However, a much smaller fraction of the astrated matter goes in massive or intermediate mass stars once the average metallicity has increased to the Population II IMF regime. Therefore, at this time, the global lithium destruction induced by astration throughout the Galaxy should decrease.

Meanwhile, the massive stars keep on enriching the ISM with metals, because they evolve rapidly. We should therefore expect a nearly constant value of the ^7Li abundance, despite the increase of metallicity or even a small increase, because of cosmic-ray ^7Li production due to spallation or moderate SNe ^7Li production. In the present framework, the slightly more lithium-poor stars observed by Bonifacio et al. (2006) and Asplund et al. (2006) around $[\text{Fe}/\text{H}] = -2.5$ mark the low-metallicity end of the lithium plateau. This may also be seen as the last stages of turbulent mixing, before the Population III SNe ejecta and the primordial ISM are mixed to the point that the early halo becomes nearly chemically homogeneous. Figure 6 illustrates the evolution we propose, once the metallicity is high enough to form Population II low-mass stars.

7.4. Final Remarks

Our scenario is still rather speculative, and has to be checked by further observational and theoretical efforts. However, we stress that a significant astration of the halo matter by Population III stars could simultaneously solve three present issues related to ^7Li : (1) the absence of this isotope in the hyper metal-poor star HE 1327-2326, (2) the apparent edge of the Spite Plateau around $[\text{Fe}/\text{H}] = -2.5$, and (3) the discrepancy between current BBN predictions of primordial lithium and the observations of lithium abundances on the Spite Plateau. A 30% to 50 % astration fraction of halo matter in Population III stars is certainly a high value (see §3). Should this astration fraction be strongly reduced, the questions raised by HE 1327-2326 and the edge of the Spite Plateau could still be related to Population III stars. One major ingredient for checking the present scenario is the chemical yields of the first stars. The rotationally-induced mixing effects have been demonstrated to explain many stellar physics features during the quiescent phase of nucleosynthesis at non-zero metallicity. These effects, as well as the explosive

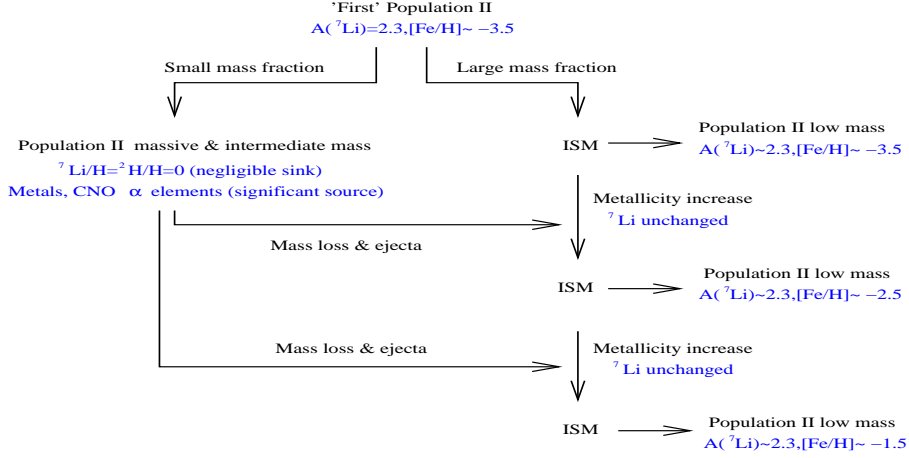


Fig. 6.— Summary of the ${}^7\text{Li}$ and metals chemical abundance evolution we suggest at the epoch of the Population II stars. At that time the IMF is probably, as now, skewed towards low-mass stars.

nucleosynthesis of the first SNe, need to be investigated further at zero metallicity. These new models should, in particular, provide an estimate of the global metal yields of the first stars in fair agreement with the observations of hyper metal-poor stars. They should also be compared with the various distinctive chemical features associated with carbon and nitrogen trends among the oldest stars of the halo. In parallel, it is important to model further the lithium evolution in hyper metal-poor stars, and to investigate the question of microscopic diffusion and gravitational settling in more detail in this environment. Additional ${}^7\text{Li}$ observations of extremely, ultra, and hyper metal-poor stars are clearly needed as well, for several reasons. First, in order to confirm or refute the possible change of slope in the $A({}^7\text{Li})$ - $[\text{Fe}/\text{H}]$ relation around $[\text{Fe}/\text{H}] = -2.5$, secondly, to inspect the ${}^7\text{Li}$ abundances for dwarf stars in the same metallicity range as HE 1327-2326. The question of whether the stars in the hyper metal-poor metallicity range are predominantly lithium poor or lithium rich would, respectively, reinforce or weaken the scenario we discuss in this paper.

Another major ingredient required for exploring the scenario we suggest is better understanding of the efficiency of turbulent mixing, and its ability to homogenize the early ISM during the time when the first generations of stars were forming. This is clearly a very complex issue given the inter-

actions between the stellar winds and ejecta, the stellar ionization effects and the interstellar magnetic fields. This point is also connected to the scenario for the formation of the Galaxy, which requires further modeling efforts. The elemental abundance patterns of the first stars can provide crucial observational clues to all of these issues. For the halo stars that exhibit $[\text{Fe}/\text{H}] > -2.5$, it is tempting to interpret the low scatter in ${}^7\text{Li}$, the α -elements, and the iron-peak elements to an imprint arising from early, efficient, mixing of the ISM. Below this metallicity, the scatter in the α -elements and the iron-peak elements remains small (Cayrel et al. 2004). The scatter in r-process elements seems to increase for metallicities below $[\text{Fe}/\text{H}] = -2$ (Truran et al. 2002). Understanding these apparently contradictory behaviors would provide crucial information about the competing efficiencies of the mixing and the stellar formation processes at the earliest epochs of the halo of the Galaxy.

If our general picture is correct, deuterium is depleted in Population II stars by at least a factor 1.5–2 below the BBN deuterium abundance. This by no means implies that half the matter of the entire Milky Way disk has been astrated in Population III stars, nor that pre-solar or local ISM ${}^2\text{H}/{}^1\text{H}$ ratio should be less than a third or a half of its primordial value. The stellar mass of the halo is roughly two orders of magnitude

below the stellar mass of the Galaxy. Moreover, the present models and observations of deuterium in the Galactic disk suggest that replenishment of this isotope has taken place, “likely from infall of gas of cosmological composition” (Romano et al. 2006). These authors predict that the deuterium fraction is constant, and near the primordial fraction, during Galactic evolution from $[O/H] = -3$ to $[O/H] = -0.5$. Since deuterium is more easily destroyed by astration than lithium, the results of Romano et al. suggests that no ${}^6\text{Li}$ or ${}^7\text{Li}$ depletion occurs in the ISM for the metallicity range of the Spite Plateau stars.

L.P. and J.W.T. acknowledge support from the National Science Fundation under Grant PHY 02-16783 for the Physics Frontier Center Joint Institute for Nuclear Astrophysics (JINA). J.W.T. also acknowledges support from the US-DOE, Office of Nuclear Physics, under contract No. W-31-109-ENG-38. T.C.B. and S.T. acknowledge partial funding for this work from grants AST 04-06784 and PHY 02-16783: Physics Frontiers Center/Joint Institute for Nuclear Astrophysics (JINA), both awarded by the U.S. National Science Foundation.

REFERENCES

- Aoki, W., Norris, J.E., Ryan, S.G., Beers, T.C., & Ando, H. 2002, *ApJ*, 576, 141
- Aoki, W., Ryan, S. G., Tsangarides, S., Norris, J. E., Beers, T. C., & Ando, H., 2003, 25th meeting of the IAU, Joint Discussion 15, 22 July 2003, Sydney, Australia
- Aoki, W., Norris, J.E., Ryan, S.G., Beers, T.C., Christlieb, N., Tsangarides, S., & Ando, H. 2004, *ApJ*, 608, 971
- Aoki, W., Beers, T.C., Christlieb, N., Norris, J.E., Ryan, S.G., & Tsangarides, S. 2006b, *ApJ*, submitted
- Aoki, W., Frebel, A., Christlieb, N., Norris, J.E., Beers, T.C., Minezaki, T., Barklem, P.S., Honda, S., Takada-Hidai, M., Asplund, M., Ryan, S.G., Tsangarides, S., Eriksson, K., Steinhauer, A., Deliyannis, C., Nomoto, K., Fujimoto, M.Y., Ando, H., Yoshii, Y., & Kajino, T. 2006a, *ApJ*, 639, 897
- Arnone, E., Ryan, S.G., Argast, D., Norris, J.E., & Beers, T.C. 2005, *A&A*, 430, 507
- Asplund, M., Grevesse, N., & Sauval, A. J. 2005, in *Cosmic Abundances as Records of Stellar Evolution and Nucleosynthesis*, eds. F.N. Bash and T.G. Barnes, ASP Conference Series Vol. 336, p. 25
- Asplund, M., Nissen, P. E., Lambert, D. L., Primas, F., & Smith, V. V. 2006, *ApJ*, 644, 229
- Avillez, M.A. & Breitschwerdt, D. 2004, *A&A*, 425, 899
- Balsara, D.S. & Kim, J.-S. 2005, *ApJ*, 634, 390
- Balsara, D.S., Kim, J.-S., Mac Low, M.-M. & Mathews, G.J. 2004, *ApJ*, 617, 339
- Barklem, P.S., Christlieb, N., Beers, T.C., Hill, V., Holmberg, J., Marsteller, B., Rossi, S., & Zickgraf, F.-J. 2005, *A&A*, 439, 129
- Bateman, N.P. & Larson, R.B. 1993, *ApJ*, 407, 634
- Ballerio, S. K., Matteucci, F., & Chiappini, C. 2006, *New Astronomy*, 11, 306
- Beers, T.C., & Christlieb, N. 2005, *ARA&A*, 43, 531
- Beers, T.C., Sivarani, T., Marsteller, B., Lee, Y., Rossi, S., & Plez, B. 2006, *AJ*, submitted
- Bonifacio, P., & Molaro, P. 1997, *MNRAS*, 285, 847
- Bonifacio, P., Molaro, P., Sivarani, T., Cayrel, R., Spite, M., Spite, F., Plez, B., Andersen, J., Barbey, B., Beers, T.C., Depagne, E., Hill, V., Francois, P., Nordström, B., & Primas, F. 2005, in *From Lithium to Uranium: Elemental Tracers of Early Cosmic Evolution*, IAU Symp. 228, eds. V. Hill, P. Francois, & F. Primas (Cambridge Univ. Press: Cambridge), p. 35
- Bonifacio, P., Molaro, P., Sivarani, T., Cayrel, R., Spite, M., Spite, F., Plez, B., Andersen, J., Barbey, B., Beers, T.C., Depagne, E., Hill, V., Francois, P., Nordström, B., & Primas, F. 2006, *A&A*, submitted

- Bonifacio, P., Pasquini, L., Spite, F., Bragaglia, A., Carretta, E., Castellani, V., Centurin, M., Chieffi, A., Claudi, R., Clementini, G., and 9 coauthors 2002, *A&A*, 390, 91
- Bouvier, J., Forestini, M., & Allain, S. 1997, *A&A*, 326, 1023
- Bromm, V., & Loeb, A. 2003, *Nature*, 425, 812
- Brun, A. S., Turck-Chièze, S., & Zahn, J. P. 1999, *ApJ*, 525, 1032
- Bullock, J. S., & Johnston, K. V. 2005, *ApJ*, 635, 931
- Burles, S. 2002, *Planetary & Space Science*, 50, 1245
- Carretta, E., Gratton, R., Cohen, J.G., Beers, T.C., & Christlieb, N. 2002, *AJ*, 124, 481
- Cayrel, R., Spite, M., Spite, F., Vangioni-Flam, E., Cassé, M., & Audouze, J. 1999, *A&A*, 343, 923
- Cayrel, R., Depagne, E., Spite, M., Hill, V., Spite, F., Francois, P., Plez, B., Beers, T.C., Primas, F., Andersen, J., Barbuy, B., Bonifacio, P., Molaro, P., & Nordström, B. 2004, *A&A*, 416, 1117
- Charbonneau, P., Christensen-Dalsgaard, J., Henning, R., Larsen, R. M., Schou, J., Thompson, M. J., & Tomczyk, S. 1999, *ApJ*, 527, 445
- Charbonnel, C., & Primas, F. 2005, *A&A*, 442, 961
- Chiappini, C., Matteucci, F., & Ballero, S.K. 2005, *A&A*, 437, 429
- Chiappini, C., Hirschi, R., Meynet, G., Ekström, S., Maeder, A., & Matteucci, F. 2006, *A&A*, 449, L27
- Chieffi, A., & Limongi, M. 2004, *ApJ*, 608, 405
- Christlieb, N., Gustafsson, B., Korn, A.J., Barklem, P.S., Beers, T.C., Bessell, M.S., Karlsson, T., & Mizuno-Wiedner, M. 2004a, *ApJ*, 603, 708
- Christlieb, N., Bessell, M. S., Beers, T. C., Gustafsson, B., Korn, A., Barklem, P. S., Karlsson, T., Mizuno-Wiedner, M., & Rossi, S. 2002, *Nature*, 419, 904
- Christlieb, N., Beers, T.C., Barklem, P., Bessell, M., Holmberg, J., Korn, A., Marsteller, B., Mashonkina, L., Mizuno-Wiedner, M., Qian, Y.-Z., Rossi, S., Wasserburg, G.J., Zickgraf, F.-J., Edvardsson, B., Gustafsson, B., Hill, V., Jonsell, K., Karlsson, T., Kratz, K.-L., Nordström, B., Pfeiffer, B., Rhee, J., & Ryan, S.G. 2004b, *A&A*, 428, 1027
- Coc, A., Vangioni-Flam, E., Descouvemont, P., Adahchour, A., & Angulo, C. 2004, *ApJ*, 600, 544
- Corbard, T., Blanc-Fraud, L., Berthomieu, G., & Provost, J. 1999, *A&A*, 344, 696
- Cyburt, R. H., Fields, B. D., & Olive, K. A. 2004, *Phys. Rev. D*, 69, 123519
- Cyburt, R. H., Fields, B. D., Olive, K. A., & Skillman, E. 2005, *Astroparticle Physics*, 23, 313
- Daddi, E., Renzini, A., Pirzkal, N., Cimatti, A., Malhotra, S., Stiavelli, M., Xu, C., Pasquali, A., Rhoads, J. E., Brusa, M., and 6 coauthors 2005, *ApJ*, 626, 680
- Dasyra, K. M., Tacconi, L. J., Davies, R. I., Genzel, R., Lutz, D., Naab, T., Burkert, A., Veilleux, S., & Sanders, D. B. 2006, *ApJ*, 638, 745
- Depagne, E., Hill, V., Spite, M., Spite, F., Plez, B., Beers, T.C., Barbuy, B., Cayrel, R., Andersen, J., Bonifacio, P., Francois, P., Nordström, B., & Primas, F. 2002, *A&A*, 390, 187
- Elmegreen, B.G. 1994, *ApJ*, 427, 384
- Ezer, D., & Cameron, A. G. W. 1971, *Ap&SS*, 14, 399
- Ferguson, J. W., Alexander, D. R., Allard, F., Barman, T., Bodnarik, J. G., Hauschildt, P. H., Heffner-Wong, A., & Tamanai, A. 2005, *ApJ*, 623, 585
- Fields, B. D., Olive, K. A., & Vangioni-Flam, E. 2005, *ApJ*, 623, 1083
- Fields, B. D. & Olive, K. A. 1999, *ApJ*, 516, 797
- Frebel, A., Christlieb, N., Norris, J. E., Aoki, W., & Asplund, M. 2006, *ApJ*, 638, 17

- Frebel, A., Aoki, W., Christlieb, N., Ando, H., Asplund, M., Barklem, P., Beers, T.C., Eriksson, K., Fechner, C., Fujimoto, M., Honda, S., Kajino, T., Minezaki, T., Nomoto, K., Norris, J.E., Ryan, S.G., Takada-Hidai, M., Tsangarides, S., & Yoshii, Y. 2005, *Nature*, 434, 871
- Gehren, T., Liang, Y. C., Shi, J. R., Zhang, H. W., & Zhao, G. 2004, *A&A*, 413, 1045
- Grevesse, N., Noels, A., 1993, "Origin and Evolution of the Elements" eds. N. Prantzos, E. Vangioni-Flam & M. Cassé, Cambridge University Press, 15
- Heger, A., & Woosley, S. E. 2002, *ApJ*, 567, 532
- Hernanz, M. Jose, J., Coc, A., & Isern, J. 1996, *ApJ*, 465, 27
- Hirschi, R. 2006, in *Proceedings of Origin of Matter and Evolution of Galaxies (OMEG05): New Horizon of Nuclear Astrophysics and Cosmology*, AIP conf. series, ed. S. Kubono, in press (astro-ph/0601498)
- Hirschi, R., Fröhlich, C., Liebendörfer, M., & Thielemann, F.-K. 2006, *Reviews of Modern Astronomy*, 19, in press (astro-ph/0601502)
- Hobbs, L. M., & Duncan, D. K. 1987, *ApJ*, 317, 796
- Inoue, S., Aoki, W., Suzuki, T. K., Kawanomoto, S., García-Pérez, A. E., Ryan, S. G., & Chiba, M. 2005, in *From Lithium to Uranium: Elemental Tracers of Early Cosmic Evolution*, IAU Symp. 228, eds. V. Hill, P. Francois, & F. Primas (Cambridge Univ. Press: Cambridge), p. 59
- Jedamzik, K. 2004, *Phys. Rev. D* 70, 083510
- Karlsson, T. 2006, *ApJ*, 641, 41
- Kawaler, S. D. 1988, *ApJ*, 333, 236
- Klessen, R.S. & Lin, D.N.C. 2003, *Phys. Rev. E*, 67, 046311
- Korpi, M.J., Brandenburg, A., Shukurov, A., Tuominen, I., & Nordlund, A. 1999, *ApJ*, 514, 99
- Lemoine, M., Vangioni-Flam, E., & Cassé, M. 1998, *ApJ*, 499, 735
- Lemoine, M., Audouze, J., Ben Jaffel, L., Feldman, P., Ferlet, R., Hebrard, G., Jenkins, E. B., Malouris, C., Moos, W., Sembach, K., and 3 coauthors 1999, *New Astronomy*, 4, 231
- Linsky, J. L. 1998, *Space Sci. Rev.*, 84, 285
- Lis, D.C., Pety, J., Phillips, T.G., & Falgarone, E. 1996, *ApJ*, 463, 623
- Lubowich, D.A., Pasachoff, J.M., Balonek, T.J., Millar, T.J., Tremonti, C., Roberts, H., & Galloway, R.P. 2000, *Nature*, 405, 1025
- Mac Low, M.-M., Balsara, D.S., Avillez, M. & Kim, J.S. 2005, *ApJ*, 627, 864
- Maeder, A., & Meynet, G. 1989, *A&A*, 210, 155
- Melendez, J., & Ramirez, Y. 2004, *ApJ*, 615, 33
- Meneguzzi, M., Audouze, J., & Reeves, H. 1971, *A&A*, 15, 337
- Meynet, G., Ekström, S., & Maeder, A. 2006, *A&A*, 447, 623
- Miesch, M.S., Scalo, J. & Bally, J. 1999, *ApJ*, 524, 895
- Molaro, P., Primas, F., & Bonifacio, P. 1995, *A&A*, 295, 47
- Montalbán, J., & Schatzman, E. 2000, *A&A*, 354, 943
- Morel, P. 1997, *A&AS*, 124, 597
- Nagamine, K., Cen, R., Hernquist, L., Ostriker, J.P., & Springel, V. 2004, *ApJ*, 610, 45
- Night, C., Nagamine, K., Springel, V. & Hernquist, L. 2005, *MNRAS*, 366, 705
- Nissen, P. E., Lambert, D. L., Primas, F., & Smith, V. V. 1999, *A&A*, 348, 211
- Norris, J. E., Ryan, S. G., & Beers, T. C. 2001, *ApJ*, 561, 1034
- North, P. 1995, *MmSAI*, 66, 395
- Oey, S. 2003, *MNRAS*, 339, 849

- Oh, S. P., Nollett, K. M., Madau, P., & Wasserburg, G. J. 2001, *ApJ*, 562, 1
- Olive, K. A., & Skillman, E. D. 2004, *ApJ*, 617, 290
- Oliveira, C. M., Hébrard, G., Howk, J. C., Kruk, J. W., Chayer, P., & Moos, H. W. 2003, *ApJ*, 587, 235
- O'Meara, J. M., Tytler, D., Kirkman, D., Suzuki, N., Prochaska, J. X., Lubin, D., & Wolfe, A. M. 2001, *ApJ*, 552, 718
- Pedlar, A., Muxlow, T. & Wills, K. 2003, *Rev Mex AA*, 15, 303
- Piau, L. 2006, *ApJ*, submitted
- Piau, L., Randich, S., & Palla, F. 2003, *A&A*, 408, 1037
- Pinsonneault, M. H., Steigman, G., Walker, T. P., & Narayanan, V. K. 2002, *ApJ*, 574, 398
- Prantzos, N. 2005, in *From Lithium to Uranium: Elemental Tracers of Early Cosmic Evolution*, IAU Symp. 228, eds. V. Hill, P. Francois, & F. Primas (Cambridge Univ. Press: Cambridge), p. 225
- Prantzos, N. 2006, *A&A*, 448, 665
- Rebolo, R., Beckman, J. E., & Molaro, P. 1988, *A&A*, 192, 192
- Reeves, H., Fowler, W. A., & Hoyle, F. 1970, *Nature*, 226, 727
- Richard, O., Michaud, G., & Richer, J. 2005, *ApJ*, 619, 538
- Ricotti, M., & Ostriker, J. P. 2004, *MNRAS*, 350, 539
- Rollinde, E., Vangioni, E., & Olive, K. 2005, *ApJ*, 627, 666
- Romano, D., Matteucci, F., Ventura, P., & D'Antona, F. 2001, *A&A*, 374, 646
- Romano, D., Tosi, M., Chiappini, C., & Matteucci, F. 2006, *MNRAS*, 369, 295
- Roy, J.R., & Kunth, D. 1995, *A&A*, 294, 432
- Ryan, S. G., & Elliott, L. M. 2005, in *From Lithium to Uranium: Elemental Tracers of Early Cosmic Evolution*, IAU Symp. 228, eds. V. Hill, P. Francois, & F. Primas (Cambridge Univ. Press: Cambridge), p. 91
- Ryan, S. G., Norris, J. E., & Beers, T. C. 1999, *ApJ*, 523, 654
- Ryan, S. G., Beers, T. C., Deliyannis, C. P., & Thorburn, J. A. 1996, *ApJ*, 458, 543
- Ryan, S.G., Beers, T.C., Olive, K., Fields, B., & Norris, J.E. 2000, *ApJ*, 530, 57
- Ryan, S. G., Gregory, S. G., Kolb, U., Beers, T. C., Kajino, T. 2002, *ApJ*, 571, 501
- Sackmann, I. J., & Boothroyd, A. I. 1992, *ApJ*, 392, 71
- Sackmann, I. J., & Boothroyd, A. I. 1999, *ApJ*, 510, 217
- Salvaterra, R., Ferrara, A., & Schneider, R. 2004, *New Astronomy*, 10, 113
- Schaller, G., Schaerer, D., Meynet, G., & Maeder, A. 1992, *A&AS*, 96, 269
- Sestito, P., & Randich, S. 2005, *A&A*, 442, 615
- Shapley, A. E., Steidel, C. C., Adelberger, K. L., Dickinson, M., Giavalisco, M., & Pettini, M. 2001, *ApJ*, 562, 95
- Simmerer, J., Sneden, C., Cowan, J.J., Collier, J., Wolff, V.M., & Lawler, J.E. 2004, *ApJ*, 617, 1091
- Sivarani, T., Beers, T.C., Bonifacio, P., Molaro, P., Herwig, F., Cayrel, R., Spite, M., Spite, F., Plez, B., Anderson, J., Barbuy, B., Depagne, E., Hill, V., Francois, P., Nordström, B., & Primas, F. 2006, *A&A*, in press
- Spergel, D. N., Verde, L., Peiris, H. V., Komatsu, E., Nolita, M. R., Bennett, C. L., Halpern, M., Hinshaw, G., Jarosik, N., Kogut, A., and 7 coauthors 2003, *ApJS*, 148, 175
- Spiegel, E. A., Zahn, J.P., 1992, *A&A*, 265, 106
- Spite, F., & Spite, M. 1982, *A&A*, 115, 357
- Spite, F., & Spite, M. 1993, *A&A*, 279, L9

- Spite, M., Cayrel, R., Plez, B., Hill, V., Spite, F., Depagne, E., Francois, P., Bonifacio, P., Barbey, B., Beers, T.C., Andersen, J., Molaro, P., Nordström, B., & Primas, F. 2005, *A&A*, 430, 655
- Suzuki, T. K., & Inoue, S. 2002, *ApJ*, 573, 168
- Thorburn, J. A. 1994, *ApJ*, 421, 318
- Timmes, F. X., Woosley, S. E., & Weaver, T. A. 1995, *ApJS*, 98, 617
- Truran, J.W., Cowan, J.J., Pilachowski, C.A. & Sneden, C. 2002, *PASP*, 114, 1293
- Tumlinson, J., Venkatesan, A., & Shull, J. M. 2004, *ApJ*, 612, 602
- Vangioni-Flam, E., Cassé, M., Cayrel, R., Audouze, J., Spite, M., & Spite, F. 1999, *New Astronomy*, 4, 245
- Venkatesan, A. 2006, *New Astronomy*, 50, 108
- Venkatesan, A., & Truran, J. W. 2003, *ApJ*, 594, 1
- Venkatesan, A., Nath, B. B., & Shull, J. M. 2006, *ApJ*, 640, 31
- Ventura, P., D’Antona, F., & Mazzitelli, I. 2002, *A&A*, 393, 215
- Ward-Thompson, D., Motte, F., & André, P. 1999, *MNRAS*, 305, 143
- Woosley, S. E., & Weaver, T. A. 1995, *ApJS*, 101, 181
- Woosley, S. E., Hartmann, D. H., Hoffman, R. D., & Haxton, W. C. 1990, *ApJ*, 356, 172
- Yan, H., Dickinson, M., Stern, D., Eisenhardt, P. R. M., Chary, R.-R., Giavalisco, M., Ferguson, H. C., Casertano, S., Conselice, C. J., Papovich, C., and 4 coauthors 2005, *ApJ*, 634, 109